On the crashworthiness performance of thin-walled energy absorbers: Recent advances and future developments

Baroutaji, Ahmad; Sajjiab, Mustafa ; Olabi, Abdul-Ghani

Published in:
Thin-Walled Structures

DOI:
10.1016/j.tws.2017.05.018

Published: 01/09/2017

Document Version
Peer reviewed version

On the crashworthiness performance of thin-walled energy absorbers: recent advances and future developments

Ahmad Baroutaji[1,*], Mustafa Sajjia[2], Abdul-Ghani Olabi[3]

(1)- School of Engineering, Faculty of Science and Engineering, University of Wolverhampton, Telford, United Kingdom, TF2 9NT

(2)- Bernal Institute, University of Limerick, Limerick, Ireland

(3)- Institute of Engineering and Energy Technologies, School of Engineering, the University of the West of Scotland, Paisley, PA1 2BE

Abstract

Over the past several decades, a noticeable amount of research efforts has been directed to minimising injuries and death to people inside a structure that is subjected to an impact loading. Thin-walled (TW) tubular components have been widely employed in energy absorbing structures to alleviate the detrimental effects of an impact loading during a collision event and thus enhance the crashworthiness performance of a structure.

Comprehensive knowledge of the material properties and the structural behaviour of various TW components under various loading conditions is essential for designing an effective energy absorbing system.

In this paper, based on a broad survey of the literature, a comprehensive overview of the recent developments in the area of crashworthiness performance of TW tubes is given with a special focus on the topics that emerged in the last ten years such as crashworthiness optimisation design and energy absorbing responses of unconventional TW components including multi-cells tubes, functionally graded thickness tubes and functionally graded foam filled tubes.

Due to the huge number of studies that analysed and assessed the energy absorption behaviour of various TW components, this paper presents only a review of the crashworthiness behaviour of the components that can be used in vehicles structures including hollow and foam-filled TW tubes under lateral, axial, oblique and bending loading.

Keywords: Energy absorbing structures, crashworthiness, impact loading, foam-filled, functionally graded thickness, multi-cell, crashworthiness design, crashworthiness optimisation, functionally graded foam material, metallic thin-walled tubes.

1. Introduction

The demand for advanced transportation in modern society is increasing on a daily basis. This has led to continuously increasing numbers of vehicles on the roads. Inevitably, vehicular crash accidents have also increased and have become a major worldwide health problem. For better safety circumstances, vehicles' structures should be able to protect occupants through converting most of the kinetic energy during a crash situation into other forms of energy in a predictable and controllable fashion. The capability of a structure to manage and absorb the force of a serious crash and to reduce death and injury risk of the occupants is known as crashworthiness [1], [2]. Thus, a crashworthy design has become the main safety criteria of the occupants-carrying vehicles such as aircraft and vehicles. The most popular form of collapsible energy absorbers, that are widely used to absorb the kinetic energy and to improve the crashworthiness behaviour of a structure, is TW components. The common use of TW components as energy absorbing devices is due to many important aspects including superior performance under dynamic loading, cost-effective, high efficiency, ease of manufacturing and installation. Thin-walled energy absorbers were employed in many applications including aircraft subfloor structures [3], front structures of cars and trains [4], Rollover Protective Structures (ROPS) of heavy equipment used in agriculture and construction, such as earthmoving machinery and tractors [5].

The principal factors that affect the energy absorption capability of such TW components are material, structural geometry and loading mode. The most used materials for manufacturing the thin-walled energy absorber are metallic, such as aluminium alloy and mild steel, and Fibre Reinforced Composites (FRCs). The energy dissipating mechanisms of metallic and composite

structures are considerably different. The structures made from composite materials are normally brittle and dissipate energy through different combined fracture mechanisms such as delamination, fibre breakage, and matrix cracking, [6], whereas the ductility nature of metallic structures allows them to dissipate energy through progressive plastic deformation.

Composite materials have gained increasing popularity in crashworthiness applications due to their high specific strength, high specific stiffness and excellent energy absorption performance. The composite structures absorb greater energy per unit mass (SEA) than the metallic structures such as mild steel and aluminium [7]. However, the design and analysis of composite energy absorbers are difficult due to anisotropic properties of composite material [8]. Also, the composite structures have an environmental effect as it is very challenging to recycle the used composite materials [8]. Additionally, the manufacturing cost of the composite materials is relatively higher than the metallic structures and this has limited their application to specific fields such as aerospace structures and race cars. Many researchers have also used hybrid structures that include both types of material, i.e. metallic and composites, to absorb a greater amount of energy such as composite wrapped thin-walled metal tubes or tubes reinforced with externally bonded fibres [9], [8], [10], [11], [12], [13], and [14]. The hybrid structures combine the desirable properties of each material, the high ratio of strength to weight of the composites and ductility and stable plastic deformation mode of the metals [11]. This paper focuses mainly on the energy absorption behaviour of metallic structures due to their common use as energy absorption devices in the vehicle body and their favourable stable plastic deformation. Expanded and detailed information on the energy absorbing behaviour of composite structures can be found in [6], [15], [1], and [16].

The energy absorbing behaviour of metallic TW tubes has received a significant amount of research in the last four decades. The main findings were reported in many review articles and books including those authored by Olabi et al [17], Alghamdi [18], Abramowicz [19], Qiu and Yu [20], Lu and Yu [1] and Jones [2]. Generally, there are various crushing or loading situations

through which metallic thin-walled tubes can be deformed plastically and absorb kinetic energy; the most common situations include axial crushing [21], lateral indentation [22]–[24], lateral compression [25], tube inversion [26]–[30], and tube splitting [31]–[36]. Each one of these crushing situations is associated with one or more deformation modes that play a main role in the energy dissipation process and lead to various energy absorption responses. Energy absorbing performance of thin-walled metallic components can be highly enhanced by using a filler material. The most common filler materials proposed in the literature include polymeric foams such as polystyrene; and metallic foams such as aluminium foam. Recently, glass fibre reinforced polyamide has been also reported in many studies as a filler material [37], [38], [39], and [40].

The design and analysis of an energy absorber are normally performed using experimental and computational techniques, such as finite element method. The computational technique is very effective and efficient tool particularly for conducting the parametric analysis. Models that can describe the energy absorption responses of structures are of great importance for analysing the performance of energy absorbing structures and they can be developed using different methods such as theoretical, empirical, and statistical methods. The theoretical models are established by observing the experimental collapse mode, simplifying the deformation mechanism, adopting some limited assumptions, and employing structural plastic analysis technique [41], [42]. On the other side, the empirical modelling is based on observations and experimentations rather than theory where the empirical expressions are derived by employing linear or nonlinear multivariable regression analysis on experimental or FE results [43], [44]. Finally, the statistical method employs the design of experiment approach for constructing an approximate model, such as response surface model (RSM), of energy absorption responses using the values of these responses at predefined sampling points [45]–[47].

In the last few years, the vehicle crashworthiness design has witnessed dramatic progress represented by using TW tubes with unconventional shape and materials as well as utilising new

techniques for analysis and optimisation of such components. The aim of the present paper is to review the energy absorbing and crush responses of the most common thin-walled components used as energy absorbers in the automobile industry. The main focus of this review is on the axial, lateral and bending deformation of hollow and foam-filled energy absorbers that made from a metallic material such as mild steel and/or aluminium. Those energy absorbers made from composite materials or crushed through inversion or splitting deformation modes are considered to be beyond the scope of this paper due to the fact that they are not commonly used for a vehicle body. This paper is structured as follows, in the first section; a complete review of the metallic energy absorbing components under axial, lateral and bending loading is given. The second section presents the foam-filled components along with the effect of filler material on the energy absorbing performance of structures. The crashworthiness optimisation methodology and various optimal configurations of thin walled structures are introduced and summarised in the third section. Finally, the opportunities for future developments in the area of structural crashworthiness are reported.

2. Hollow thin-walled energy absorber (HTWEA)

2.1 Dynamic Behaviour of Metallic Materials

The crash components of a road vehicle are mostly manufactured using a metallic material such as aluminium alloy and mild steel. Aluminium structures are considered very effective for developing the lightweight vehicle.

The mechanical properties of the absorber's material, such as yield stress and strain hardening behaviour, play an important role in the crashworthiness behaviour. Metallic materials are normally sensitive to loading rate where their mechanical properties under dynamic loading are different from those observed under quasi-static loading. It should be noted that the material's strain rate sensitivity is a material property and is independent of the geometrical factors of the TW tube [2]. The dynamic behaviour of metallic materials has been substantially investigated and

almost a complete understanding has been established. A summary of the studies and findings on the dynamic response of materials that are most relevant to the crashworthiness topic is presented in Table 1. It is evident from this table that the plastic behaviour of the most metallic materials including mild steel, aluminium and magnesium alloys is highly sensitive to strain rate. Such materials exhibit an increase in yield and ultimate stresses as the strain rate increases. The strain rate sensitivity behaviour of a material manifests itself as a strengthening effect in a TW component [2]. It has been considered that material strain rate sensitivity is a beneficial phenomenon since it allows the material to achieve a greater energy absorption capacity when it is loaded dynamically [2]. In practice, strain rate effects are usually included in the analysis by using dynamic plastic flow instead of static plastic flow stress. The dynamic plastic flow stress could be calculated using a Cowper-Symonds equation as follows

$$\sigma_d = \sigma_s \left(1 + \left(\frac{\dot{\varepsilon}}{D} \right)^{\frac{1}{q}} \right) \qquad 1$$

where σ_d is the dynamic flow stress, σ_s is the static yield stress, $\dot{\varepsilon}$ is the strain rate, the constants D and q are parameters of the material.

Understanding the dynamic behaviour of material is essential for formulating or selecting a proper constitutive equation which can describe the indispensable relation between the strains and the stresses; and can be implemented in a numerical code for modelling purposes. Various constitutive models for the strain-rate-sensitive behaviour of materials have been proposed in the literature. The main constitutive equations that are applicable to metallic materials include Cowper-Symonds model, Johnson-Cook model, Zerilli–Armstrong (ZA) model, Bodner–Partom (BP) model, Khan–Huang (KH) model. Many experimental tests are required in order to obtain the various coefficients in these constitutive equations. A detailed review of these constitutive models was introduced by Liang and Khan [48].

2.2 Loading situation

The geometrical shape of a TW tube and the way through which it is loaded and deformed are crucial factors in the crashworthiness performance. These factors determine the amount of the tube's materials that undergoes plastic deformation and participate in the energy absorbing process. Basically, the most common loading situations of the thin-walled tubes used in the protection system of a road vehicle are axial, oblique, lateral and bending loading, Figure 1. As an example, during a full frontal collision scenario, the front longitudinal rails including the crash boxes undergo axial deformation mode and absorb around 50% of the total kinetic energy where the crash box itself accounts for around 15% of the total absorbed energy [49]. On the other side, the bumper cross beam undergoes a bending or lateral deformation mode and absorb around 25% of the total energy [50]. The remaining kinetic energy is absorbed by the other front structural components of the vehicle such as front panel, fenders, wheel wells, and hood.

2.2.1 Axial loading

Axially loaded TW components are the most commonly used structures as energy absorbers and appear mainly in the crash box behind the car bumper. The axial crushing of tubes is characterised by a reasonably constant collapse load and a comparatively high energy absorbing capacity where the specific energy absorbing capacity of axially loaded components is approximately 10 times greater than that in laterally compressed tubes [18]. This is basically due to the fact that under axial loading, the majority of the tube's material deforms plastically to participate in the energy dissipating process. The axially loaded energy absorbers have a huge variation in terms of geometric shape where they may be: circular, square, triangle, or polygon in cross-section. Furthermore, they may be formed in a single or multi-cell configuration. Additionally, they may adopt a form that is straight or tapered in appearance. The energy absorbing behaviour of various cross-sections and configurations of axially loaded components were compared in many papers and a summary of these is presented in Table 2. The crush behaviour and deformation modes of the main shapes are reviewed in detail below.

2.2.1.1 Circular and Square Tubes

The axial crushing of circular tubes was extensively studied by many researchers [51], [52], [53], [54] for its energy absorption capability. Those authors were among the first researchers who developed an analytical model for the axial collapse of a circular tube. The axial crushing of a circular tube involves progressive folding or buckling of the tube with one or more of three main deformation modes: axisymmetric or ring, non-symmetric or diamond, or a mixed mode as shown in Figure 2.

The geometry of a circular tube, represented by the ratio of diameter to thickness (*D/t)* and the ratio of length to thickness (*L/t)*, was reported to have a significant influence on its deformation mode during axial crushing [21]. Broadly speaking, the diamond mode occurs in tubes with *D/t* greater than 80 while the ring mode occurs when *D/t* is less than 50 and *L/t* is less than 2. For tubes with *D/t* less than 50 and *L/t* bigger than 2, mixed mode is developed [1].

Many researchers developed theoretical models for each deformation mechanism of the axial crushing of the circular tubes. A summary of the most famous theoretical models that predict the mean crush force (*MCF*) of the circular tubes is tabulated in Table 3. For the sake of convenience, researchers such as Guillow et al. [21], who investigated the axial compression of circular aluminium tubes under quasi-static conditions, developed an empirical expression for mean crush force that works for any deformation mode. The developed empirical formula relates the mean crush force to *D/t* ratio as shown in equation *2*

$$MCF = 18.075\sigma_o t^2 \left(\frac{D}{t}\right)^{0.32} \qquad 2$$

In addition to geometrical parameters, loading velocity has a great influence on the deformation mode of a circular tube. The influence of impact velocity on the deformation pattern was investigated by Wang and Lu [55]. Cylindrical shells were subjected to axial impact with velocities values of up to 300 m/sec. It was found that high impact speeds produced a unique plastic deformation called ‘Mushrooming’ which made the walls of the shell thicker. The authors

identified three modes of deformation, as shown in Figure 3, depending on the velocity of impact and the thickness of the tubes as follows: (i) progressive deformation mode in the form of folds for tubes with small wall thickness at relatively low velocity, (ii) mushrooming associated with folds for all tubes at medium velocity, and (iii) mushrooming associated with wrinkling for tubes with big wall thicknesses at high velocity.

In practice, the use of circular components in the automobile structures met various difficulties associated with mounting to other structural members. Thus, for addressing the practical issues, square tubes have received a noticeable attention for fabrication of crashworthy components.
Generally, the square tubes are less effective at absorption energy than circular tubes. Tang et al [56] reported that the structural effectiveness of a square tube is about 0.7 of a circular tube. This could mainly be due to the fact that severe deformation in square tubes is concentrated in the zones near to the corner. Similar to the circular tube, the cross-section dimensions play an important role in the deformation mode of square tubes. The collapse mode depends on the width to thickness (*b/t*) ratio and it could be either extensional mode, inextensional, or mixed [2], as shown in Figure 4. A very thin square tube, typically with $b/t \approx 100$, may adopt a non-compact deformation mode, Figure 4-d.
Regardless the deformation mode, the mean crush force of axially crush square tube is given by equation 3 as derived by Wierzbicki and Abramowicz [57]

$$MCF = 9.56\sigma_o b^{1/3} t^{5/3} \qquad 3$$

Abramowicz and Jones [52] updated the last equation into equation 4 to take into account the strain hardening effect

$$MCF = 13.06\sigma_o b^{1/3} t^{5/3} \qquad 4$$

In general, based on their dimensions, the thin-walled tubes can undergo a global buckling or global bending deformation mode during their axial crushing. This mode is very inefficient and

should be avoided when designing an energy absorption structure because it is relatively unstable and can lead to a considerable decrease in the effectiveness of an energy absorber. The global bending deformation mode may occur in both square and circular tubes as shown in Figure 5. The occurrence of global bending in axially loaded circular tubes depends on the diameter to thickness (D/t) and length to diameter (L/D) ratios, as reported by Guillow et al [21]. The experimental results obtained by Abramowicz and Jones [58], who investigated the transition of mild steel circular and square tubes from the inelastic global Euler buckling mode to the progressive folding mode, showed that there is a critical tube length (L_{cr}) where the tubes with lengths less than the critical value deform progressively while tubes longer than the critical length undergo a global bending mode. When the tube's length is close to critical value, a mixed progressive deformation-global bending deformation mode was observed where the global bending mode developed at the later stages of the deformation. Generally, the transition criterion, i.e. the critical length, is believed to be influenced by the following factors: material properties including the yield stress and strain hardening behaviour, impact velocity, and tube dimensions [58], [59], [60], [61], [62]. Abramowica and Jones [58] reported that square tubes with greater b/t or circular tubes with greater D/t have longer L_{cr}. Karagiozova and Alves [61] found that L_{cr} increases as the impact velocity increase.

2.2.1.2 Frusta and tapered thin-walled tubes

Frusta and tapered TW tubes which include one or more inclined face to the longitudinal axis and may have circular, rectangular or square cross-sectional shape were also considered as energy absorbing components by many researchers [44], [63]–[71]. Generally speaking, the tapered tubes are preferable to the straight (non-tapered) tubes due to their capability of absorbing the oblique impact loads effectively where they are less likely to undergo the global buckling mode. Also, the tapered tubes have more stable plastic behaviour and lower initial peak force under axial loading than the non-tapered tubes. Additionally, from a design point of view, tapered tubes,

with an additional design variable represented by the semi-apical angle, have a bigger design space and thus they can offer better energy absorption characteristics than the straight tubes.

The energy absorption behaviour of tapered tubes depends mainly on the geometrical factors including the cross-sectional shape, wall thickness and taper angle [72]. Nagel and Thambiratnam [44] found that the specific energy absorption (SEA) of a tapered tube with square cross section is less than that of a straight tube and they reported that in the applications where weight is important and reducing weight is a goal, straight tubes are favoured and represent the most effective structure for absorbing energy. Guler et al [72] compared the energy absorbing behaviour of tapered and straight TW tubes with circular, square and hexagonal cross sections and found that a tapered tube with circular cross section is the most efficient energy absorber among the studied sections.

The deformation modes of tapered tubes are similar to those of straight tube where circular tubular cones usually deform in either the diamond mode or concertina mode, depending on the geometry of the tube [64].

2.2.1.3 Multi-Corner tubes

It was mentioned in section 2.2.1.1 that the severe deformation in the square tubes occurs in the zones near the corner. Intuitively, introducing more corners in the cross-section of TW tube lead to more plastic deformation and hence more energy dissipation. Thus, multi-corner TW tubes have attracted increased attention as energy absorbing components for a wide range of applications including automobiles, shipbuilding and civil engineering [73]–[77].

In most studies, energy absorption enhancement was reported for TW with hexagonal and octagonal sections. For example, Abramowicz and Wierzbicki [78] derived the mean crushing forces of hexagonal tubes as

$$MCF = 20.23\sigma_o b^{0.4} t^{1.6} \qquad 5$$

By benefitting from equation 4, it is evident that the hexagonal tube has higher mean crush force than a square tube with the same outer perimeter.

The common progressive deformation modes of the regular multi-corner tube are the same as those reported for square tubes, i.e. inextensional, extensional and mixed modes [79].
The angle between the side walls of a multi-corner tube determines to a large extent the deformation behaviour of the multi-corner tube. The common trend is that the acute angle adopts inextensional deformation mode while extensional deformation mode is developed when the angle is higher than 120^{o}. Mixed deformation mode which consists of extensional and inextenstional folding lobs was observed for the angle from 90^{o} to 120^{o} [75]. It has been identified that the highest crushing energy absorption efficiency can be achieved when the angle between the neighbouring flanges is in the range from 90^{o} to 120° [56], [80].

Although increasing the number of corners in the regular multi-corner columns seems to be a promising approach to enhance the energy absorption behaviour, some researchers observed that energy absorption improvement almost saturates for the number of corners beyond 11 [81]. This behaviour may be due to the fact that regular multi-corner convex columns are unable to satisfy the condition of both increasing the number of corners and maintaining the angle between neighbouring flanges in the optimal range [80]. To overcome these limitations, researchers suggested introducing inward corners to generate columns with concave cross-sections such as star [82] and criss-cross sectional tube [80], [83], [84]. Abbasi et al [83] studied the collapse behaviour of an innovative 12-edge criss-cross sectional tube and proved its superior crashworthiness performance; in terms of greater specific energy absorption (SEA) and crush force efficiency (CFE); over conventional convex profiles such as square, hexagonal, octagonal columns. Fan et al [82] compared the energy absorbing capability of concave polygonal sections including 12-sided and 16-sided star cross-sectional columns with more conventional convex sections including octagon and hexagon profiles. The authors noticed that the 12-sided star cross

section displayed the best energy absorption performance with an increase of up to 48.5% in the SEA compared with the hexagon cross section of the same cross-sectional area. The energy absorption capacity of 16-sided star cross section was lower than that of 12-sided one which suggests that increasing the number of corners is not always effective even in columns with concave sections.

The other way to breakthrough the limitation of multi-corner cross-section with a large number of corners is by inserting angle elements (internal webs) in the cross section [56]. The crush behaviour of an angle element is influenced by the number of panels and the angle between neighbouring flanges where SEA increases as the number of panels increases [75].

2.2.1.4 Triangular tubes

The majority of the research studies have been focused on the TW tubes with an even number of sides. Meanwhile, little attention has been paid to the axial crushing of polygonal tubes with an odd number of sides, such as triangular tubes [75], [85]–[88]. The triangular cross-section has only three corners (three sides) and hence it exhibited the least energy absorbing capacity among all other tubes. Its progressive folding is quite unique and different from those developed in the multi-corner tube [86].

The collapse mechanism of equilateral triangular structures under quasi-static axial loading was analysed by Fan el al [86]. Two main deformation modes were recognised for these structures based on their dimensions, named as rotational symmetrical mode observed in tubes with $c/t > 60$, and diamond mode, for tubes with $c/t \leq 55.3$. The theoretical models for calculating the mean crushing forces are given in equations 6 and 7 for diamond and rotational deformation modes, respectively [86]. These models provided satisfactory predictions for the crushing load in case of diamond mode while it couldn't predict the same for the rotational mode [86].

$$MCF = 0.25\,\sigma_o t^2\,(15.561 + 15.052\sqrt{c/t}) \qquad 6$$

$$MCF = 0.25\,\sigma_o t^2\,(12.038 + 17.126\sqrt{c/t}) \quad (7)$$

where t and c are the thickness and side length of the triangular tube

Due to the fact that the energy absorbing capability of such tubes is quite low, they did not receive much application in the automotive industry.

2.2.1.5 Multi-cell Tubes

It is been identified in section 2.2.1.3 that inserting an angle element in a TW tube is a feasible method to overcome the limitation associated with increasing the number of the corner in a multi-corner tube. The structural member generated from a combination of angle elements with TW tube is called as a multi-cell or cellular tube. The energy absorption efficiency of a multi-cell TW tube depends to a large extent on the number of angle elements in the cross-section. The mean crush force of a multi-cell square tube, as shown in Figure 6, was derived by [89] and is given for a quasi-static as in equation 8

$$MCF = \sigma_o t\sqrt{(N_c + 4N_o + 2N_T) \times \pi \times L_c \times t} \quad (8)$$

Where N_c is the number of corners, N_0 the number of criss-crosses and N_T the number of T-shape cross-sections, and L_c is the total length of the walls of the cross-section. It is clear that MCF increases as the number of angle of elements increases, i.e. number of cells, and this proves the expected energy absorption enhancement that could be achieved by using the multi-cell configuration of the TW tube.

The multi-cell configurations was applied to the various cross-sectional shapes including hexagonal [46], triangular [41], square [42], [90]–[94], circular [56], [95], [96] octagonal [85], and tapered [97] tubes. The studies on the multi-cell tubes have revealed that these structures are very weight-effective components with extraordinary energy absorption capability. For example, Xiong and Hui [91] reported that multi-cell metal tubes, S4 and S 5 in Figure 7, are more efficient

than single-cell tubes. An increase of 120% and 220% were recorded in the specific energy absorption for specimens S4 and S5 respectively. Zhang and Cheng [98] performed a comparative analysis of energy absorbing responses of multi-cell and foam-filled square tubes. The authors proved via numerical simulations that the multi-cell components are effective energy absorbers where their energy absorption efficiency was about 50–100% larger than that of foam-filled tubes. Alavi Nia and Parsapour [85] presented an interesting investigation in which they compared the energy absorption capacity of conventional and multi-cell TW tubes with octagonal, hexagonal, square, triangular cross-sections. The authors proved that the tubes with multi-cell configuration have higher energy absorbing capacity than the tubes with standard sections. Furthermore, the multi-cell tubes with octagonal and hexagonal cross sections were found to have the highest specific energy absorption. Kim [99] studied the crashworthiness behaviour of multi-cell square tubes with four different shapes. Theoretical models for calculating the mean crush force for each configuration was derived. The results revealed that the SEA increased with the number of cells and around 100% gain in SEA could be achieved in multi-cell tubes. Table 4 presents the mean crush force and the gain in SEA for the various multi-cell tubes.

2.2.1.6 Functionally graded thickness (FGT) tubes

The functionally graded thickness is a novel idea that aims to change the materials distribution within a TW tube to achieve desirable energy absorption goals such as greater plastic deformation and SEA, lower initial peak load, or less tendency to undergo global bending mode. In these components, the thickness gradient represents an additional design variable that improves the designability and allows for better use of material for meeting the requirements of vehicular light weight [100].

The concept of FGT has been presented to various shapes of TW energy absorbing components such as square tubes [100], circular tubes [101] and frusta [102], [103]. For circular tubes and frusta, the wall thickness was varied in the longitudinal direction, as shown in Figure 8-

a, to achieve a lower peak load at the beginning of crush [102], [103]. On the other side, the thickness in square tubes was varied in the transverse direction, as demonstrated in Figure 8-b, to place more material in the corners of the square section which undergo a severe deformation during the axial loading [104].

The FGT thin-walled components have better designability and crashworthiness behaviour than their counterparts with a uniform thickness [102], [103]. As an example of the effectiveness of FGT energy absorbers, Xiong et al [100] studied the crush and energy absorbing behaviour of square tubes with a graded thickness. The authors reported that the specimen with graded thickness can absorb 30–35% more energy per unit mass than the normal specimen, i.e. specimen with uniform thickness, without increasing the initial peak force.

2.2.1.7 Unconventional thin-walled components

During their endeavour to design a TW tube with better energy absorbing capability, researchers and engineers devised many unconventional structural members with complicated cross-section and a unique loading situation. Some of those innovative and promising structures are presented in this section.

2.2.1.7.1 Biaxial buckling of TW tubes

Menouer et al [105] suggested a new form of energy absorption structures based on biaxial buckling. A complex deformation mode was generated using a unique mechanical system that transforms an axial loading into combined compression–torsion biaxial one. Copper and annealed aluminium alloy tubes with circular and square cross-sections were used. The results obtained from this investigation revealed that the biaxially deformed tubes, as shown in Figure 9, exhibited greater mean collapse load and energy absorption than the uniaxially deformed components with an increase in the absorbed energy reached up to 47% when inclination angle was 60^{o}.

2.2.1.7.2 TW tubes with stiffeners and corrugations

Stiffened tubes, in which external stiffeners is used with a circular tube, as shown in Figure 10-a, were considered as efficient energy absorbers [106]. These components exhibited several improvements in the crush energy absorbing behaviour such as high energy absorption capacity, better crushing stability and less sensitive to loading characteristics such as direction and uniformity [106]. Most of these improvements were achieved through the capability of externally stiffened tubes to develop an axisymmetric deformation mode during the axial collapse where the plastic deformation occurred in the regions between the stiffeners and the stiffeners worked as a stabilisation tool for the whole structure

Similar to stiffened tubes, researchers also evaluated corrugated tubes as effective energy dissipating devices. Introducing corrugations in the axially loaded tubes forced the plastic deformation to take place at specific places along the length of the tube. This behaviour enhanced the uniformity of the force–displacement response and allowed for predicting and controlling the collapse mode of the tubes [107]. Arameh et al [108] conducted an experimental study into the energy absorption performance of aluminium tubes with corrugations that were varied in geometries and directions, as shown in Figure 10 (b and c). The authors observed that tubes with corrugations had improved crashworthiness characteristics, uniform crush responses without high initial peak loads, and predictable collapse mode. They reported that corrugated tubes with their predictable energy absorption performance can be considered as reliable energy absorbers.

2.2.1.7.3 Thin-walled tubes with triggers and cut-outs

The force-displacement response of the axially loaded thin-walled tubes is attributed by an initial high peak force followed by lower peaks corresponding to each fold generated during the progressive collapse, Figure 5-c.

When designing an axially loaded energy absorber, it is always desirable to minimise the initial peak force as the high peak force could cause serious negative effects. As such, crush triggers,

also called collapse initiators, stress concentrators, or imperfections, have been traditionally introduced in the axially loaded absorbers to reduce the peak forces. The crush trigger can be defined as a slight modification in the conventional shape of thin-walled tubes such as indentations in the sidewalls, holes and windows, dents and so on [109]. The crush triggers assist in the deformation of TW tube because they raise the initial stresses when the tube is loaded [110]. Also, these triggers can be used to encourage the symmetric deformation mode, even if the tube's geometry would normally cause another mode of failure, which has more stable crush response and better energy absorption performance [109].

Applying of a trigger mechanism in the thin-walled tubes has created non-standard configurations of the energy absorption devices. Some examples of using triggers in the thin-walled energy absorbers are presented below while a full review of the different types of triggers and their effects on the deformation modes and behaviour of tubular energy absorbers is available elsewhere [109].

Gupta and Gupta [111] introduced cut-outs in a form of circular holes to aluminium circular tubes. It was noticed that the tubes with cut-out holes exhibited lower initial peak load during the axial collapse. The authors reported that using the cut-outs provided the benefit of a greater deformation stroke before the beginning of global bending mode.

Song et al [112] presented thin-walled square tubes with rectangle windows. It was pointed out that introduction of windows has reduced the weight of the tube while maintained its mechanical properties. It was found that introducing the windows in the square thin walled tubes enhanced the crushing behaviour with 54% as the maximum increase in the specific energy absorption (SEA) and 63% as the highest decrease in the initial peak load under quasi-static loading condition.

Guler et al [72] and Taştan et al [113] have proved the effectiveness of introducing cut-outs on the crashworthiness behaviour of tapered TW tubes. It was shown that frusta tubes with cut-outs

outperform the normal tubes with an increase of 26.4% and 27.4% for SEA and CFE, respectively [113].

2.2.2 Oblique loading

Since the axially loaded tubular structures can be used for vehicle crashworthiness applications in which the crush management system is frequently subjected to both oblique and straight loads, many investigations have been performed to analyse and evaluate the energy absorbing behaviour of various TW components under oblique loads. Safety requirements for vehicles demand that the frontal protection system (bumper) should be designed to endure an oblique load with an angle of up to 30^{o} to the longitudinal axis [114]. Generally, the oblique loading causes the tube to bend while undergoing some form of progressive folding which will eventually develop to a global bending mode, Figure 11.

The early investigation presented in this regard was performed by Reid and Reddy [63]. Tapered rectangular tubes were subjected to oblique impact load with an angle of 10^{o} to the tube's longitudinal axis. The results showed that the energy absorbing effectiveness of tapered tubes was almost same for both oblique and axial loads. The previous work was expanded by [69] who examined the effects of loading parameters, including the impact velocity and the load angle, and the geometry variables, including the taper angle, number of tapered sides, wall thickness, web width and tube length, on the behaviour of tapered and straight TW rectangular tubes under oblique dynamic loading. The authors reported that the tapered tubes exhibited many important benefits over straight tubes including more stable mean load, greater energy absorbing capacity when the tube underwent a global bending deformation mode, and energy absorption characterizations with less sensitive to load parameters. Reyes et al [115], [116] studied the energy absorbing behaviour of aluminium square tubes under dynamic and quasi-static oblique loads. It was observed that the dominant deformation mode under the oblique loading was global bending which depended on both load angle and thickness. The authors also confirmed that the mean and peak loads decreased as the loading angles increased. Furthermore, the authors reported

that there was no change in collapse mode between the quasi-static and dynamic cases. Børvik et al [117] investigated the crush response of circular aluminium tubes under quasi-static oblique loading. It was also observed that both energy absorption and peak force decreased with increasing the loading angle.

The responses of other geometrical shapes of obliquely loaded TW energy absorbers were also reported in the literature. The studied cross-sections included multi-cell hexagonal columns [46], frusta [118], [119], empty and foam-filled square tubes [120], multi-cell square tube [42], [90], tapered square tubes [69], [121]. The main observation that was reported by the researchers is that the TW components under oblique loading are more likely to undergo the global bending deformation mode which may extremely reduce its energy absorption effectiveness. The tendency of the tube to undergo a global bending mode increases with increasing the loading angle.

Despite the aforementioned studies, the energy absorption responses of TW tubes subjected to oblique loads have received relatively little attention compared to the number of studies conducted on the crush behaviour of TW tubes under straight loads.

2.2.3 Lateral loading

The lateral collapse of TW tube involves compressing or flattening the entire length of the tube parallel to its longitudinal axis. This deformation mode could be developed for the cross-beam of car bumper under front impact situation and thus the flattening process was the subject of many research studies. The laterally crushed energy absorbing systems may consist of a single tube or may take the form of nested tube system in which many tubes are stacked together to satisfy specific requirements.

2.2.3.1 Circular tube

The circular tube is the most investigated shape under lateral loading; its crush behaviour and collapse mechanism under lateral compression have been well studied in the literature [25], [122]–[128]. Many theoretical models were developed by [122]–[124] for the crushing of a circular tube compressed laterally by flat plates. The most accurate model was the one proposed

by Reid and Reddy [124] in which geometric and material strain-hardening effects were considered. A simple deformation mechanism of a laterally loaded circular tube involves generating four stationary plastic hinges, as shown in Figure 12. The lateral compression load of a short-length circular tube is derived by [122], as follows

$$F = \frac{2\,\sigma_Y\,t^2\,L}{D\left[1-\left(\frac{\delta}{D}\right)^2\right]^{1/2}} \qquad 9$$

The geometrical parameters of a circular tube govern its deformation mode and energy absorption behaviour in case of quasi-static/low impact loading. The mean crush force and the energy absorbing capacity of the laterally crushed circular tube increase with decreasing the diameter and increasing the thickness [25], [129].

The behaviour of a circular tube under dynamic lateral loading was studied by [128], [130], [131]. Under impact loading, the impact velocity is the dominant factor of the collapse pattern while tube dimensions have an insignificant effect on the deformation pattern [131]. In general, no change in the deformation mode or energy absorption capability was reported for tube crushed under low impact velocity [130]. However, under high impact velocity, a laterally crushed circular tube shows a noticeable increase in the amount of absorbed energy and significant change in the deformation mode [130]. This behaviour is mainly due to inertia effects which localise the plastic strains close to the striking side and increase the curvature of the segment subjected to deformation [130].

The plastic deformation in a laterally crushed circular tube is confined to zones near the plastic hinges generated during the collapse and thus the amount of energy dissipated through the lateral collapse of a tube is limited and inefficient. Therefore, in order to increase the amount of energy absorbed during the lateral collapse, researchers suggested using external constraints, including vertical-shaped sides [132] and V-shaped sides [133], or bracing wires [134] to create more plastic hinges during the compression. A constrained tube was first introduced by Reddy and

Reid [132] who used vertical side constraint to prevent the horizontal diameter of a laterally loaded circular tube from becoming greater. It was found that a constrained tube offer higher energy absorption capacity and lower deflection distance than the unconstrained tube. A different form of external constraints was used by Reid [133], who employed inclined constraints (V-shaped block) to increase the number of plastic hinges. It was noticed that the crushing force increased as the angle of 'V' block decreased. Reid et al [134] suggested a different method to enhance the energy absorbing of the laterally collapsed tube. They used tension members across the diameters of a tube to create a braced tube with the desired response. A noticeable enhancement in the energy absorbing responses was reported for such tubes.

2.2.3.2 Other cross-sectional shapes

In addition to circular tubes, tubes with various cross-sectional shapes such as elliptical [135]–[137], rectangular [138]–[140], hexagonal [141], oblong [142] and triangular [143]–[145] were also investigated under lateral loading in the literature.

Generally, a square tube absorbs more energy than a rectangular tube with the same cross-sectional area [138]. The deformation mechanism of a square tube under lateral loading involves generating three pairs of plastic hinges, as demonstrated in Figure 13, two pairs are formed at junctions of vertical and horizontal sides while the last pair is formed at the mid-height of the vertical sides of the tube [138] and [139]. The collapse load of a square tube is given by equation 10, as derived by [139]

$$F = \frac{2\,\sigma_0\,t^2\,L\,cos^{-1}((b-\delta)/b)}{\delta} \qquad 10$$

Similar to the circular tube, the geometrical parameters of a square tube are the main factors which influence its energy absorption behaviour. The results obtained by Niknejad et al [139], who investigated the lateral collapse of rectangular brazen and aluminium columns under quasi-static loading, revealed that the specific absorbed energy by a rectangular column increases as the column thickness increases and width decreases.

Niknejad and Rahmani [141] studied the lateral crushing of hexagonal columns under quasi-static loading. A plastic deformation mechanism which consists of 6 plastic hinges at the corners of the hexagonal section was adopted in this study to extract the crushing force of the section. It was found that lateral load of the tube is proportional to the width and thickness of the tube.

Wu and Carney [136] investigated the lateral compression of elliptical tubes. It was found that the crush efficiency and energy absorbing capacity of an elliptical tube are greater than those of the circular tube.

Baroutaji et al [142] reported on the lateral compression of oblong tubes. An oblong structure was formed by elongating the standard circular tube plastically in the diametrical direction as shown in Figure 14. The results of this investigation showed that an oblong tube exhibited more stable crush response and greater energy absorbing capacity than a circular tube of equivalent mass.

Wang et al [143] examined the lateral crushing and energy absorption behaviour of triangular tubes under quasi-static lateral loading. The results demonstrated three main crushing styles of such tubes based on the base angle. Tubes with small base angle, less than 45.6°, crushed without folds, as depicted in Figure 15-a, while tubes with big base angle, greater than 72.6°, were folded, as illustrated in Figure 15-c. Tubes with a base angle between 45.6^{o} and 72.6^{o} have the crushing pattern as illustrated in Figure 15-b. A plastic hinges mechanism, as shown in Figure 15-d, was adopted to derive the mean crushing force of these tubes.

It should be noted that the available data in the literature don't allow comparing the energy absorption behaviour of the various structures under lateral loading. Also, the research work that reports on the mean crush force of such structures is very rare and thus more theoretical and comparative analysis is required for these structures.

2.2.3.3 Nested tubes

As mentioned before, the energy absorption capacity is limited in a laterally loaded tube. Thus, in order to meet the design requirement of some applications which require larger energy absorbing capacity, Many researchers [146]–[150] suggested that the tubes can be stacked together to form a tubular system with desirable energy absorption behaviour. The nested systems are of particular importance for applications with limited crush zone as they have more than one crushable element in the same space and thus they can absorb higher energy per unit length than a single tube [147].

Among the early investigations in this regards, Morris et al [149] proposed nested tube systems in which circular or oblong tubes of different diameters were assembled and compressed by rigid platen under quasi-static lateral loading as shown in Figure 16-a. As it can be seen from the figure, these nested systems contain gaps between their components which caused sequential deformations for their components which in turn caused a non-monotonic rise in force throughout the deformation distance. An attempt was made by Olabi et al [148], [151] to optimise the responses of the previous systems by inserting two small bars in the space between the nested tubes, as shown in Figure 16-b. The authors pointed out that using the small bars in the optimised configuration of nested systems was able to eliminate a *non-monotonic* increase in the force-displacement response that was noticed during the collapse of the standard nested systems. It was found that the optimised nested system displayed a more desirable crush response than the normal system. Another attempt to improve the response of the nested tube system was introduced by Baroutaji et al [147]. Baroutaji et al [147] arranged the components of nested systems in particular ways, as shown in Figure 16-c, so that they deformed synchronously upon loading in order to achieve the desirable force-deflection response. The authors reported that a nested tube system with two identical inner tubes (middle system in Figure 16-c) exhibited the best energy absorption performance. The energy absorption capability of the nested system can be enhanced

significantly by applying the concept of external constraints as demonstrated by Morris et al [150] who analysed the responses of constrained nested systems, as shown in Figure 16-d. It was found that the nested systems with external constraints absorbed more energy than those without external constraints.

2.2.4 Bending loading

Since many of car components at the front, rear and side, such as B-pillar, side-door beam, cross-beam of the bumper, may fail in bending mode during a collision, investigating the bending behaviour of TW components is required when designing a vehicle body.

Studying the bending collapse of TW tubes is much more complicated than axial response due to the fact that the bending strength is significantly influenced by the shape, size and location of the loading punch [152]. Bending collapse or lateral indentation of tubes involves applying a point load perpendicular to the longitudinal axis of the tube, as shown in Figure 1. The deformation of TW component under bending starts with a local indentation at the location of loading followed by a global bending of the tube due to a significant reduction of the cross section area at the loading location, Figure 17. The mean crush force of a square tube under bending loading was derived by Wierzbicki et al [153] as

$$MCF = 2.76\sigma_o b^{1/3} t^{5/3} \qquad 11$$

By using equations 4 and 11, one can clearly see that the axial loading yields *MCF* that is almost 5 times greater than bending loading.

The cross-sectional shape of the TW member influences its energy absorption behaviour under bending loading. Tang el al [154] compared the bending performance of different cross sections including circular, rectangle, ellipse, trapezoid and hat section under dynamic loading. It was found that the elliptical tube was harder to be deformed into a flat shape in the plastic hinge zone and thus it exhibited better energy absorption behaviour than the other tubes.

The energy absorption through bending can be greatly enhanced by adopting the multi-cell configuration [152]. Wang et al [152] investigated the bending collapse of the multi-cell square tube. The multi-cell configuration of TW was introduced in the longitudinal direction and in the cross-section. The multi-cell configuration in the longitudinal direction was created using partition plates. These plates were found to be effective when one plate was located beneath the punch. On the other side, the multi-cell configuration in the cross-section was found to enhance the bending resistance. A tube with double-cell in the cross-section exhibited higher energy absorbing measurements than the other configurations and it was considered as the most effective multi-cell tube under bending loading.

Introducing a graded thickness configuration in the TW tube is another way to enhance the resistance of a structure under bending loading [155]- [156]. Zhang et al [155], who studied the bending response of FGT square tubes, reported that functionally graded thickness tube offers 40 % increase in SEA than the uniform tube under bending loading. Sun et al [156] analysed the bending response of TW tube with a circular section and a thickness gradient along the longitudinal direction. It was proved that FGT provides better crashworthiness behaviour than the uniform tube.

Using ribs in the thin-walled beam was also identified as an effective way to improve the bending response [154], [157]. The ribs help in retarding the local deformation at the loading location resulting in improving the bending and energy absorbing performance [154].

3. Foam-Filled thin-walled energy absorber (FFTWEA)

Of interest for HTWEA is to improve their crashworthiness performance while maintaining a minimum mass. One approach for this is to use a lightweight material such as a fibre reinforced polyamide [37]–[40], cork [158], [159], wood [160], polyurethane foam [161], carbon nano polyurethane foam [162], and metal foam [163] as a filler material in TW tubes. These filler

materials deform largely at almost constant crushing load and thus using them along with TW tube enhances the energy absorbing behaviour of the filled tube.

3.1 Dynamic behaviour of Foam material

Among all types of filler materials, metallic and polymeric foam materials have received increased attention as a new generation of lightweight materials with high potential for enhancing energy absorption characteristics and stabilising the crush response of a structure. The weight and structural efficiencies of the filled structures make them practical for engineering applications as in passenger vehicles.

It is well-established in the literature that the mechanical behaviour of a foam depends on the cell microstructure (cell size, cell topology, etc.), properties of the metal and the relative density of the cellular material [164]. The effect of cell microstructure on the behaviour of foam materials is basically due to fact that the deformation mechanism of foam material at cell level is governed by bending and stretching of cell wall followed by buckling and tearing in post-yield stage [165]. The cell wall bending strength is affected by the cell size where the smaller cell size exhibited higher strength due to increasing strength of cell edges [166]. Since the mechanical behaviour of cellular materials is influenced by the cell microstructure, the morphological imperfections in cell microstructure such as non-uniform cell wall thickness, cell-size variations, fractured cell walls, cell-wall misalignments, and missing cells were found to have a significant effect on the mechanical behaviour of the metallic foams [167].

Generally, the mechanical properties of the cellular material are a function of the foam relative density [163]. The mechanical strength of foam material increases with increasing the relative density due to an increase in the bulk material within the foam [168]. This behaviour can be expressed mathematically as a power law relationship between the plateau stress (σ_f) and foam relative density (ρ_f/ρ_{fo}) as shown in equation 12

$$\sigma_f = C_f \left(\frac{\rho_f}{\rho_{fo}} \right)^n \qquad 12$$

Where ρ_f is the foam density and ρ_{fo} is the density of the base material. C_f and n are material constants which can be obtained by model calibration to uniaxial compression test data for foam cubes [163].

The dynamic response of a cellular material is different to its quasi-static counterpart due to strain rate effect. The strain rate sensitivity of cellular material increases with increasing the relative density of the cellular material [169]. The macroscopic strain-rate sensitivity of the cellular material are attributed to many sources as follows [170]

- The strain rate sensitivity of foam material may be due to the inherent strain rate sensitivity of the base material that forms the cell-wall as reported by [171]
- The strain rate sensitivity of foam material may be due to effects of micro-inertia or inertia of the individual cell walls in dynamic buckling of cell walls of the cellular material. Tan et al [172] reported that, in the case of moderate strain rate, the closed-cell aluminium foam with small cell size is more sensitive to strain rate than that with big cell size due to increased micro-inertial effects in the smaller cells.
- The strain rate sensitivity of foam material may be due to the contribution of the pressure of the entrapped air in honeycombs as discussed in [173]
- The strain rate sensitivity of foam material may be due the shockwave effects that may be generated in case of intensive impact load (high strain rate) and cause a dynamic localisation of the crushing, as reported by the Reid and others [172], [174], [175]

The role of each of the aforementioned sources on the dynamic response is generally unclear and consensus on that has not been achieved yet. A detailed review of the mechanical and dynamic behaviour of foam materials is beyond the scope of this paper; nonetheless, some of the important findings on the dynamic behaviour of the most relevant foam material to the topic of the paper are summarised in Table 5. Expanded and essential background about the dynamic behaviour of the

cellular material is available in a review paper by Reid et al [176] and book by Gibson an Ashy [165].

The computational modelling of the dynamic behaviour of foam materials can be performed by two approaches: macro-mechanical and micromechanical methods, Figure 18. The macro-mechanical approach treats foam as a bulk continuum and requires a constitutive model that describe the elastic-plastic behaviour of the of foam material under loading. Over the years, various constitutive models of metallic foams have been developed. Hanssen et al [177] evaluated the main constitutive models that are implemented in the commercial FE package such as LS-DYNA and reported that none of them can predict the behaviour of metallic foam materials with convincing accuracy. This is mainly due to fact that these models don't consider the local or global fracture of the foam which is likely to be occurred during the crushing process. Additionally, none of these models can account for the change of foam's density, i.e. compressibility, during the crushing [178]. Developing new constitutive models that account for the fracture and compressibility of foam material is vital for improving the accuracy of crash simulations of foam materials. On the other hand, the micromechanical approach considers the microstructure of a real cellular solid. The micro-mechanical models have evolved from simple models with idealised cell geometries and microstructures; such as Kelvin cell models; to more sophisticated random models obtained using the Surface Evolver software [179]. The micromechanical models of foam material can overcome the limitations reported for macro-mechanical models and can provide more accurate predictions for the crushing behaviour of such materials.

3.2 Axial Loading

The early investigations on the crashworthiness of FFTWEA were performed by Reid et al [180], [181] in which a polyurethane foam was used as a filler material in square, rectangular and tapered tubes subjected to dynamic and quasi-static axial loading. Extensive research has been performed later to study the energy absorbing behaviour of such tubes with different shapes, as

seen in Figure 19, including square tubes [182], [183], [184], [185], hexagonal and octagonal tubes [184], circular tubes [117], [186], [187], [188], tapered rectangular tubes [189], conical tubes [43], [119], [161], and hat sections [190], [191], [192]. All of these studies reported significant enhancements in the crashworthiness behaviour of the FFTWEA.

In general, FFTWEA provides better crush response, higher weight efficiency, greater energy absorption and less tendency for global bending than HTWEA [181], [193], [194], [183], [195]. The deformation mode in FFTWEA tends to be compact mode with a higher number of folds [182], [196], as seen in Figure 20. Also, the diamond deformation mode in an empty circular tube alters to a concertina mode in a foam-filled tube, regardless of the foam type and density [182], [196], Figure 21. These changes in deformation mode of foam-filled tubes are mainly due to the interaction effects between the thin-walled tube and the filler material [1]. The interaction effects in the foam-filled components are attributed to two reasons; first, the presence of foam-filler inside a TW component produces more resistance to outward and inward folding and thus the plastic fold wavelength reduces and the number of folds increases during the progressive axial collapse; and second, the interfacial friction stress between the filler material and the tube wall [182] and [187]. The aforementioned interaction effects make the crush force of the foam-filled tube higher than the sum of the crush forces of empty tube and foam when they are crushed separately [185], as seen in Figure 22. Considering the interaction effects, many analytical models were developed for assessing the mean crush force of FFTWEA. A summary of these models is presented in Table 6.

The density of a filler material in foam-filled components is the most influencing factor that controls the crush and energy absorbing behaviour of FFTWEA. Generally, A FFTWEA with higher foam density exhibits higher energy absorption capacity [189], [197]. However, increasing the foam density over an optimal value may lead to many serious consequences such as global bending deformation mode, low weight effectiveness, and premature tensile rupture [198], [181], [1], [98], [199]. For example, Reid et al [181] found that using polyurethane foam with a density

of higher than 320 kg/m^3 may cause global bending in foam-filled square tubes. Seitzberger et al [198] noticed that using an aluminium foam with a density of 0.7 g/cm^3 in foam filled circular tubes can cause global bending, as shown in Figure 23. The author suggested that using foam density of lower than 0.6-0.7 g/cm^3 may prevent global bending characteristics in foam-filled circular tubes. The results obtained by Onsalung et al [197], who investigated the energy absorption behaviour of a square steel tube filled with polyurethane foam, indicated that a filled tube with a foam density of 200 kg/m^3 offers higher specific energy absorption than a tube with a density of 300 kg/m^3. Thornton [200] and Thornton et al [201] found that that weight effectiveness tends to be reduced in a polyurethane foam-filled when the foam density was higher than 220 kg/m^3.

3.3 Oblique Loading

The performance of foam-filled tubes was also evaluated under oblique loading in many studies [114], [117], [119], [120], [202]–[204].

Generally, the energy absorption parameters including peak load and mean load of foam-filled tubes decrease significantly with increasing the load angle [114], [117]. The global bending mode is the predominant mode for such components which causes a huge reduction in the energy absorption capacity [117], [204]. The foam density has an effect on the crashworthiness behaviour of foam-filled tube under oblique loading where the higher foam density yields higher specific energy absorption and higher peak loads [120]. However, the foam-filled components with higher foam density undergo a global bending mode under a smaller loading angle [204].

The general trend for the foam-filled tubes is that the foam doesn't provide any advantage for crashworthiness behaviour under oblique loading and the empty tubes outperform the filled ones under such loading condition [114], [117], [120]. One solution for the poor crashworthiness performance of FFTWEA under oblique loading could be to replace the straight tubes with conical tubes. Ahmad et al [119], who examined the energy absorbing responses of empty and polyurethane foam-filled conical TW components under oblique impact loading, found that foam-

filled conical tubes can effectively absorb both oblique and axial impact loads and they have a less tendency to undergo a global bending deformation mode. The authors reported that the global bending mode can be avoided using conical tubes with semi-apical angle bigger than 5^{o}. The foam in such components produces greater resistance to bending rotation enabling these components to exhibit less tendency for global bending mode [119].

3.4 Lateral Loading

The crashworthiness performance of various shapes of foam-filled thin-walled structures under lateral loading, as shown in Figure 24, was also reported in the literature [45], [141], [205]–[207].

Niknejad et al [207] performed an experimental study on the lateral crushing of brazen circular tubes filled with polyurethane foam under quasi-static loading. The experimental results revealed that using polyurethane foam enhanced the energy absorption properties of the circular tubes under lateral loading where the foam filled tubes exhibited higher energy absorption than the empty ones.

Laterally compressed hexagonal columns were investigated by Niknejad and Rahmani [141]. Empty and polyurethane foam-filled tubes manufactured from a brass alloy, steel, and galvanised iron materials were tested under quasi-static lateral loading. It was demonstrated that the foam-filling has an effect on the lateral collapse of such column where the lateral load increased by increasing the plateau stress of the filler material.

Fan et al [208] conducted an experimental investigation on the lateral compression of sandwich tubes made of aluminium alloy and ALPORAS® aluminium foam. Three types of deformation mechanisms were observed in the lateral collapse of sandwich tubes as follows: sequential collapse pattern, simultaneous collapse pattern, and simultaneous collapse pattern with fracture of the foam core. The results showed that sandwich tubes have enhanced crush strength and energy absorption behaviour.

Fan et al [130] reported on the dynamic lateral crushing of sandwich structures. The results revealed that when the sandwich structures were subjected to an impact velocity lower than a certain value, called as critical impact velocity, they exhibited comparable deformation modes and energy absorption measurements to those observed in the case of quasi-static loading. While, when an impact velocity higher than the critical is used, sandwich tubes absorbed a greater amount of energy than that absorbed in the quasi-static case.

Niknejad and Orojloo [209] studied the lateral collapse of nested foam-filled tubes systems with a special cross-section, as shown in Figure 24-d. Aluminium alloy was used for the grooved section while aluminium alloy and brass alloy were used for the inner circular tube and polyurethane foam was used as a filler material. Experimental investigations were performed to explore the effect of loading angle, filler material, material of the inner tube and nesting arrangement on the response of the system. The obtained results indicated that a nested system consisted of grooved section and polyurethane foam-filled aluminium tube and oriented according to zero loading angle situation has the highest specific energy absorption.

Overall, as it can be seen from the abovementioned studies, the foam filling can be also considered an effective way to enhance the energy absorption behaviour under lateral loading. The main reason for the energy absorption enhancement is the greater plastic deformation occurred at the contact zones between the tube and the loading plates.

3.5 Bending Loading

The crush and energy absorption responses of foam-filled TW structures subjected to bending loading were investigated for square [210], [211] and circular [212], [213] sections. As found in the other deformation modes, filling the TW component with a foam material enhanced the bending strength significantly and improved the energy absorbing performance of the filled structure.

Generally, the presence of foam plays an important role in delaying the local indentation by introducing additional support from inside [212]. Also, the interaction effects represented by friction between the foam filler and tube wall make the crushing loads of foam-filled tube greater than the sum of the individual crushing loads of the foam and the TW tube [213].

However, in such components, the tube wall may suffer from tensile failure, as shown in Figure 25, that significantly reduces the energy absorption capability [213]. The tensile failure depends mainly on foam density where it happens quicker in the tubes filled with higher foam density [213]. So a careful selection of the foam density is required to extract the maximum crashworthiness of these structures.

3.6 Advanced Foam-Filled Components

3.6.1 Functionally graded Foam

The studies mentioned above on the FFTWEA used foam materials with uniform densities that are supposed to have approximately identical microscopic cells, isotropic and homogeneous material characteristics. Although the superior energy absorbing enhancement observed for such tubes, the uniform foam may not be the best option of the materials for maximising the crashworthiness performance. Thus, recently, many interesting investigations used a new form of filler material called as functionally graded foam (FGF) material in which the density is not uniform and has a gradient in either axial or lateral direction. From a design viewpoint, the density gradient is an additional design variable which guarantees a wider design domain and a better designability.

Generally, producing a FGF material is more complicated than fabricating a uniform foam due to the varying material properties; however, many researchers [214]–[216] have developed new technologies that allowed for creating such materials under laboratory conditions. The functionally graded foam materials were first fabricated by Gupta [217], and Gupta and Ricci [218] where the experimental results reported by the authors showed that FGF material has an

enhanced energy absorption performance. Another confirmation on the better performance of FGF as energy absorption material was reported by Cui et al [219] who examined FGF with micro-scale cells that were changed continuously in a particular fashion. The authors reported that the FGF materials are promising candidates for enhancing energy absorption properties over those classic foam materials. Many recent studies have reported on using FGF as a filler material to enhance the crashworthiness of TW structures with different shapes including circular tubes [101], multi-cell square columns [220], square tubes [221], tapered circular tubes [222]. All results obtained from these investigations indicated that FGF-filled thin-walled tube has better energy absorption performance than uniform foam-filled components.

The density gradient could be either in the transverse or longitudinal direction. The crush and energy absorbing performance of FGF were found to be insensitive to the gradient direction but they were sensitive to whether the density is an increasing or decreasing function in the gradient direction [223]. The FGF with ascending density gradient, from the impacted surface to the opposite surface for longitudinal FGF; or from the tube's centre towards the circumference for the transverse FGF, exhibited improved energy absorbing behaviour compared to those FGF with descending gradient density [219], [224], [225].

3.6.2 Honeycomb filler

Metal and composite honeycomb structures were introduced as a filling core in many studies [199], [226], [227]. A honeycomb-filled tube exhibited improved crashworthiness performance and higher energy absorption measurements than a hollow tube under axial loading [199], [226]. Santosa and Wierzbicki [199] reported that filling a TW component with aluminium honeycomb is more weight efficient than using aluminium foam filling. This is mainly due to the fact that the honeycomb has a lower density than aluminium foam for the same volume and therefore it offers higher strength to weight ratio than aluminium foam. Hussein et al [226], who conducted an experimental investigation on the axial crushing of square aluminium tubes filled with polyurethane foam and/or aluminium honeycomb, founded that a polyurethane foam-filled tube

yields higher energy absorption measurements than a honeycomb-filled tube and thus it was concluded that polyurethane foam core is more effective than honeycomb filling.

The honeycomb filling was also used for enhancing the crashworthiness behaviour of square tubes under bending loading [211]. It was reported that the honeycomb filling is preferable to increasing the thickness of the tube and the honeycomb-filled tube absorbs higher specific energy absorption than the aluminium foam-filled tube under the bending loading [211]. The energy absorption behaviour of honeycomb can be further enhanced by adopting a functionally graded configuration for the core [228]. The main advantage of such filling is the ability to improve the energy absorption capability without increasing the peak crush force [228]. Zhu et al [228] reported on the crashworthiness response of double functionally graded (DFG) structure, which consists of a functionally graded thickness (FGT) tube filled with functionally graded honeycomb, under multiple loading cases. It was found that DFG showed greater energy absorption capacity than the hollow tube and the tube filled with normal honeycomb.

3.6.3 Auxetic Foam

Auxetic foam, which is a new generation of foam material, has been used as a filler material in TW tubes [229]. This foam material exhibits a unique mechanical behaviour under compression or extension loads in which it is contracted transversely when compressed longitudinally and vice versa. This behaviour is due to the fact that Auxetic foam has a negative Poisson's ratio.

The crashworthiness effectiveness of Auxetic foam was investigated by Mohsenizadeh et al [229] who studied the axial collapse of aluminium square columns filled with Auxetic foam. The results of this investigation proved that the Auxetic foam-filled components have higher energy absorption, higher SEA, and better progressive collapse than the empty and polyurethane foam-filled tubes.

4. Crashworthiness design and optimisation

Basically, the major challenge in the design and development of an energy absorbing component is how to find an optimal sectional configuration of a thin-walled tube that satisfies best the crashworthiness requirements.

Traditionally, the design cycle of a crashworthy structure, as shown in Figure 26, starts with choosing the geometrical shape of the section which is normally determined by the space constraints and other functions required from the component. Following the selection step, crashworthiness performance of the section is assessed by considering the main responses including the deformation mode, mean crush force, and peak crush force. In order to achieve the best crashworthiness design, the design cycle, Figure 26, should be repeated many times and this demands a quick assessment of the proposed design.

In recent times, various optimisation techniques, such as multi-objective particle swarm optimisation (MOPSO) algorithm, genetic algorithm and desirability approach, have received increased application in the area of structural crashworthiness by researchers and engineers to seek for optimal crashworthy design.

4.1 Crashworthiness design criteria

Selection of proper design criteria is crucial for getting an effective optimal design. The main indicators that can represent the crashworthiness behaviour of thin-walled components and were most presented in the literature are specific energy absorption (*SEA*), energy absorption (*EA*), mean crush force (*MCF*), peak crush force (*PCF*), crush force efficiency (*CFE*), effective crush distance (d_{eff}), energy efficiency (E_E), and crush efficiency (S_E), Table 7.

Different design criteria were used when finding the optimal shape. Some of those criteria are very confusing and used paradoxically by researchers. For example, some studies [230], [231] considered that the optimal design should have a long effective crush distance to allow for a complete utilisation of the plastic deformation, while others [232], [233] suggested that the optimal design should have a short effective distance to avoid the severe intrusion of the engine

booth into survival space [234]. *MCF* was also used in a contradictory way in the optimisation studies where some researchers [185], [235] suggested low levels for MCF to reduce the injuries risk and others [236] maintained high MCF to increase the energy absorption capacity. However, the reason behind the paradoxical use of some crashworthiness metrics might be linked to the safety regulations of the automotive structures which generally fall into two main groups with one focus on the static criteria, such as deformation, and the other emphasis the dynamic criteria such as impact or acceleration [237].

The most agreed design criteria are those that use the *SEA* and *PCF* parameters. The energy absorber should dissipate the maximum possible amount of energy per unit mass, in order to allow for a lightweight design with efficient fuel consumption, so the *SEA* was selected as an objective function and maximised in the most crashworthiness optimisation studies. On the other side, the crushing of the energy absorber during a crash scenario should not lead to high decelerations felt by the occupants in the survival space to avoid the severe injury or death that may happen to them. This aim can be achieved by maintaining as low *PCF* as possible. Thus, *PCF* is considered as a safety indicator for the vehicle and passengers and was selected as an objective function in many crashworthiness optimisation problems and minimised.

4.2 Mathematical formulations of crashworthiness metrics

In order to use the common optimisation techniques, the designer of the absorption structure needs first to describe the various crashworthiness parameters mathematically. One obvious way for this is to develop analytical models for the crashworthiness responses such as *SEA* [99] and *MCF* [41], [42]. However, the energy absorption behaviour of the structures under various loading conditions is one of the highly nonlinear mechanic problems and hence it is very complicated to establish analytical solutions for this behaviour.

Thus, design of experiments (DOE) approach is normally adopted by researchers to construct surrogate models such as radial basis functions (RBF) [238], response surface (RS) [129], support vector regression (SVR) [222], artificial neural network (ANN) [230], [231], [239], and kriging

(KRG) [90] models which relate the crushing and energy absorption responses to various design variables for analysis and optimisation purposes.

The surrogate model of a crashworthiness response, such as (RSM), is a mathematical expression that relates the design response to controllable input variables. The design variables could be one or more of the geometrical parameters, material parameters and loading parameters. The advantage of employing the surrogate model as an analysis and optimisation tool in the field of energy absorption systems is that the energy absorbing behaviour of a structure in a particular design space can be identified by performing a limited number of experiments at the sampling design points or training points. DOE offers a set of methods to construct the sampling design points such as factorial, Box–Behnken (BBD) [129], [142], central-composite (CCD), fractional factorial design (FFD) [240], D-optimal [45], the optimal Latin Hypercube sampling (OLHS) [113], Taguchi or orthogonal arrays (OA) [239], and so on.

After selecting the design type, experiments are conducted at the design points and the crashworthiness responses are calculated. Since experiments are expensive and time-consuming, numerical simulations are widely employed by researchers and engineers to conduct parametric studies. The computational modelling of thin-walled tubular structures is frequently performed using finite element models. The FEM is a very effective tool in the field of design and development of energy absorbers as it provides much more detailed information than the experimental methods.

It is worth to mention that no consensus has been reached by researchers on the most appropriate surrogate model for the crashworthiness design [239]. Additionally, it was reported that the most accurate surrogate model doesn't always lead to best optimal solutions [113], [240]. Thus, it is recommended that more than one surrogate model should be adopted in the optimisation algorithm to obtain multiple optimum candidates and then a decision can be made on the candidate that has best crashworthiness performance.

4.3 Formulation and solving of crashworthiness optimisation problem

The general mathematical formulation of crashworthiness optimisation problem is

$$\begin{cases} Minimise\ f(x) = [f_1(x), f_2(x), \dots., f_i(x)] \\ s.t \quad g(x) = [g_1(x), \dots, g_i(x)] \leq 0 \\ x^l \leq x \leq x^u \end{cases} \qquad 13$$

Where $x=(x_1,x_2,\dots,x_k)$ is the vector of k design variables, x^L and x^u are respectively the lower and upper bounds of the design variables, *f(x)* and *g(x)* are the objective function and the constraint function, respectively. The design variables *(x)* can be selected to represent on or more of geometrical, material and loading parameters, while the objective and constraint functions represent the different crashworthiness responses, such as *MCF* and *SEA*, and can be formulated based on surrogate modelling.

Generally, the optimal design of an energy absorber can be sought by following one of two main frameworks; single-objective optimisation approach or multi-objective optimisation design. In the single-objective framework, only one primary design response, such as *SEA* or *PCF*, is considered as an objective function in the formulation of the optimisation problem which tries either to maximise or minimise this response based on specific design requirement. The other less important responses are prescribed as functional constraints.

The single-objective optimisation framework was used in many crashworthiness designs [163], [195]. However, this approach is not fully suitable for crashworthiness because the reliable crashworthiness design requires considering all crashworthiness responses simultaneously. Also, it is difficult even for an expert crashworthiness engineer to identify which response is a primary objective and what constraints should be imposed to those less important responses.

For these reasons, it is more meaningful to formulate the crashworthiness optimisation problem within multi-objective optimisation framework, which considers more than one objective and

capable of providing more information on the interaction between the different crashworthiness responses.

Typically, the solutions of the multiobjective optimisation problem can be obtained by two methods. One is to investigate each of the objective functions independently and find all possible optimal solutions that known as the Pareto optimal solution. There are many optimisation algorithms that can be used to generate 'Patero optimal' solutions such as Multiobjective Particle Swarm Optimisation (MOPSO) algorithm [220], [241], [242], Non-Dominated Sorting Genetic Algorithm (GA-II) [243], [244], Genetic Algorithm (GA) [245] and so on.

On the other hand, the second solution method combines all objective functions into one function called as cost objective function and seeks for only one solution for the optimisation problem. The second method can be applied by using weighted average method [246] or desirability approach [45], [129].

Since the crashworthiness design of energy absorption components might involve some degree of uncertainties in many aspects such as material properties, geometries and loading, robust and reliable design approaches were used to formulate the crashworthiness optimisation problem in many studies [247]–[250]. The robust design approach considers the stochastic of design variables and responses by combining the mean value and standard deviation in the objective functions as follows

$$\begin{cases} Minimise & F(\mu_f(x), \sigma_f(x)) \\ s.t & g(x) \leq 0 \\ & x^l \leq x \leq x^u \end{cases} \quad 14$$

Where μ_f and σ_f denote mean value and standard deviation of objective functions, respectively.

The reliable design approach uses probabilistic constraint functions to avoid falling in the infeasible region when uncertainties present. The reliable design approach can be formulated as

$$\begin{cases} Minimise & f(x) \\ s.t & P(g(x) \leq 0) \geq R_t \\ & x^l \leq x \leq x^u \end{cases} \quad (15)$$

where R_t is the reliability level and $P(\cdot)$ is the probability of the constraints functions

The detailed theoretical information about the various optimisation strategies that can be used in structural crashworthiness is beyond the scope of the paper and they are available elsewhere [234].

4.4 Summary of optimisation researches

Extensive researches have been conducted to find the optimal crashworthiness design of the various TW tubes, a summary of these studies with a focus on cross-section shape, geometrical modification, loading situation and filling condition is shown in Table 8.

The use of crashworthiness optimisation techniques was not limited to finding the optimal shape of a simple TW tube but also it is expanded to include finding an optimal design of a complete part or system for automotive industry such as car door [250], car bumper beam [251], vehicle roof structures [252], vehicle front body structure [253], vehicle full body structure [247], [254]–[257], vehicle restraint system [258], vehicle side [259], frontal energy absorbing structure of subway vehicle [260], and railway vehicle driver's cab [261].

5. Future Directions

The ultimate goal of the research work in the crashworthiness domain is to develop a lightweight design that has efficient fuel consumption while maintaining effective crashworthiness performance under a crash scenario. This aim has been achieved partially by using lightweight materials, such as aluminium and magnesium alloys. From a review of the literature, it was found that aluminium alloy is becoming a worthy material for consideration in the domain of crashworthiness while magnesium alloys have received limited interest. So, it is

anticipated that more research work will be done to investigate the crashworthiness behaviour of magnesium structures in order to fully realise the advantages that can be gained from using these structures as energy absorbing systems.

It was shown in this review that the axially loaded components, that absorb energy through progressive deformation, are very effective energy absorption devices. However, the progressive deformation is very challenging as the axially loaded components may develop an inefficient deformation mode, known as global bending mode, for certain dimensions. The global buckling mode for circular and square components have received sufficient consideration while other configurations including components with multi-cell, multi-corner and FGT have received no attention. Investigating the global buckling phenomena of such configurations should provide the designer with a wider scope for a proper selection of the effective energy absorber and thus, it is also recommended for further investigation.

Among all shapes of TW structures used for energy absorption purposes, the tapered components have shown superior performance in which they were able to absorb the oblique loading as effective as they absorbed the axial loading. The tapered components with circular or square cross sections have received a considerable amount of studies in the literature. The other possible sections including polygonal section have received no research work and this could be another dimension for future research activity in the area. These components are promising energy absorber as they can benefit from the higher number of corners and sides for increasing the energy absorbing capacity and from the tapering configuration for enhancing the crashworthiness performance under oblique loading.

The concept of functionally graded structures showed a notable enhancement in the crashworthiness performance. The main focus of the previous studies in this regards was on circular and square sections. Multi-corner tubes with thickness gradient have received very limited attention and thus they could be a very promising topic for future research.

The complete energy absorbing structures used in the automotive industry consist of components that deform axially and laterally. The lateral collapsing of thin-walled structures has received relatively less attention than axial deformation. It is recommended that more attention should be dedicated to investigating the lateral and bending collapse of innovative structures such as those with multi-cell configuration and graded thickness that exhibited a superior performance under axial loading.

From reviewing the optimisation researches, it was found that most of the studies have focused on the behaviour of a solo thin-walled and a little attention was directed towards analysing a complete energy absorbing system. However, in order to provide reliable design recommendations, the effectiveness of an optimised TW component should be verified when it is assembled with other structural components to build a complete energy absorbing system.

Finally, it was demonstrated in this review that the response of cellular materials to dynamic loading is a complicated behaviour and the microstructure constituents of the foam including the shape and size of cells have a significant effect on this behaviour. Thus, in order to attain a comprehensive understanding of collapse mechanisms of such materials during an impact scenario, the microstructure evolution must be captured and understood. The recent micromechanical computational models are capable of reproducing all aspects of the microstructural deformation behaviour and could assist in understanding the mechanical properties of cellular materials when it subjected to dynamic loading. Thus, it is suggested that such techniques should receive more attention in future crashworthiness studies in order to understand the dynamic behaviour of such structures.

6. Summary

The vehicle accidents are among the leading causes for death worldwide as they are responsible for more than 1.3 million fatalities and around 39 million injuries annually. Thus, the

vehicle structural integrity (Crashworthiness) has gained more attention in academic design research and the automotive industry to prevent injury and ensure the safety of occupants in an event of a collision.

The impact energy absorbers in a vehicle' structure consist of TW components that can be deformed either axially (crushable columns behind the bumper) or laterally (cross-beam of the bumper) or in bending mode (B-pillar, doorsill beam, cross-beam of the bumper).

The axially collapsed TW components provide higher energy absorption than those collapsed laterally or in bending. This is mainly due to the fact that under axial loading most of the tube's volume reach the plasticity limit and participate in the energy absorption process. The energy absorbed by the axial collapse showed a significant dependence on the tube geometries and an absorber with circular cross section was reported as the most efficient shape in many studies. In spite of their excellent energy absorption performance, the axially loaded tubes might adopt an undesirable deformation mode, termed as global bending, which is unstable and causes an extreme reduction in the energy absorbing capacity. This deformation mode is most likely to appear in the long tubes and under oblique loading situation. The TW members crushed laterally or in bending mode showed less energy absorption than the axially loaded components. This is mainly due to deformation mode developed under such loading, i.e. plastic bending, which restricts the plastic deformation to a limited volume of the material.

Modifying the geometry shape of the energy absorber was always considered as an effective method for enhancing the crashworthiness behaviour of the components. New unconventional configurations of thin-walled tubes including multi-cell components and functionally graded thickness tubes were extensively studied for their application as energy absorbers. The goal of multi-cell configuration is to improve the energy absorption behaviour of TW tube by controlling the number and shape of angle elements in the cross section. Functionally graded thickness configuration aims to increase the amount of material at the locations that suffer from a serious

deformation while reducing the amount of material at less important zones and hence it allows for better distribution of tube's material. Both configurations of TW components exhibited greater crashworthiness measurements and enhanced energy absorption behaviour than the conventional tubes for all loading situations. However, the multi-cell tubes are not widely used in practice due to high manufacturing cost and high peak crush force of such structures. In addition to modifying the shape of the TW component, using a filler material in a TW tube is the classical route to enhance its energy absorption performance. The foam-filled TW tubes absorb higher energy than empty tubes due to the interaction effects between the filler material and the thin-walled tubes along with the energy absorbed by the filler material itself. A new form of foam material with a density gradient was recently developed and considered for crashworthiness applications. The functionally graded foam materials showed better crashworthiness responses than the conventional foam material with uniform density due to their ability to increase the specific energy absorption without increasing the peak crush force.

Traditionally, the design of TW energy absorber was performed by theoretical and experimental methods that are expensive, time-consuming and limited to TW tube with a simple shape. The recent significant developments in the computational resources helped the researchers and engineers to use new tools for the crashworthiness design, represented by the integrating of finite element simulations with the surrogate modelling and optimisation techniques (as reported in section 4). These tools have empowered the automotive industry to avoid the complete reliance on hardware prototyping, reduce the development costs and shorten the time to the market.

7. References

[1] G. Lu and T. X. Yu, *Energy Absorption of Structures and Materials*. Elsevier, 2003.

[2] N. Jones, *Structural Impact*. Cambridge University Press, 2011.

[3] C. Bisagni, "Crashworthiness of helicopter subfloor structures," *Int. J. Impact Eng.*,

vol. 27, no. 10, pp. 1067–1082, Nov. 2002.

[4] J. Marsolek and H.-G. Reimerdes, “Energy absorption of metallic cylindrical shells with induced non-axisymmetric folding patterns,” *Int. J. Impact Eng.*, vol. 30, no. 8–9, pp. 1209–1223, Sep. 2004.

[5] Z. Ahmad and D. P. Thambiratnam, “Application of foam-filled conical tubes in enhancing the crashworthiness performance of vehicle protective structures,” *Int. J. Crashworthiness*, vol. 14, no. 4, pp. 349–363, Jul. 2009.

[6] A. G. Mamalis, M. Robinson, D. E. Manolakos, G. A. Demosthenous, M. B. Ioannidis, and J. Carruthers, “Crashworthy capability of composite material structures,” *Compos. Struct.*, vol. 37, no. 2, pp. 109–134, Feb. 1997.

[7] S. Ramakrishna and H. Hamada, “Energy Absorption Characteristics of Crash Worthy Structural Composite Materials,” *Key Eng. Mater.*, vol. 141–143, pp. 585–622, Sep. 1998.

[8] K. C. Shin, J. J. Lee, K. H. Kim, M. C. Song, and J. S. Huh, “Axial crush and bending collapse of an aluminum/GFRP hybrid square tube and its energy absorption capability,” *Compos. Struct.*, vol. 57, no. 1–4, pp. 279–287, Jul. 2002.

[9] H.-W. W. Song, Z.-M. M. Wan, Z.-M. M. Xie, and X.-W. W. Du, “Axial impact behavior and energy absorption efficiency of composite wrapped metal tubes,” *Int. J. Impact Eng.*, vol. 24, no. 4, pp. 385–401, Apr. 2000.

[10] E. H. Hanefi and T. Wierzbicki, “Axial resistance and energy absorption of externally reinforced metal tubes,” *Compos. Part B Eng.*, vol. 27, no. 5, pp. 387–394, Jan. 1996.

[11] M. R. Bambach, M. Elchalakani, and X. L. Zhao, “Composite steel–CFRP SHS tubes under axial impact,” *Compos. Struct.*, vol. 87, no. 3, pp. 282–292, Feb. 2009.

[12] M. R. Bambach and M. Elchalakani, “Plastic mechanism analysis of steel SHS strengthened with CFRP under large axial deformation,” *Thin-Walled Struct.*, vol. 45,

no. 2, pp. 159–170, Feb. 2007.

[13] Z. Ahmad, M. R. Abdullah, and M. N. Tamin, “Experimental and Numerical Studies of Fiber Metal Laminate (FML) Thin-Walled Tubes Under Impact Loading,” in *Advanced Structured Materials (Edited by Andreas Öchsner and Holm Altenbach)*, vol. 70, A. Öchsner and H. Altenbach, Eds. Cham: Springer International Publishing, 2015, pp. 433–443.

[14] R. D. Hussein, D. Ruan, and G. Lu, “Cutting and crushing of square aluminium/CFRP tubes,” *Compos. Struct.*, vol. 171, pp. 403–418, 2017.

[15] J. J. Carruthers, A. P. Kettle, and A. M. Robinson, “Energy Absorption Capability and Crashworthiness of Composite Material Structures: A Review,” *Appl. Mech. Rev.*, vol. 51, no. 10, p. 635, Oct. 1998.

[16] A. G. Mamalis, D. E. Manolakos, G. A. Demosthenous, and M. B. Ioannidis, *Crashworthiness of Composite Thin-Walled Structures*. CRC Press, 1998.

[17] A. G. Olabi, E. Morris, and M. S. J. Hashmi, “Metallic tube type energy absorbers: A synopsis,” *Thin-Walled Struct.*, vol. 45, no. 7–8, pp. 706–726, Jul. 2007.

[18] A. A. A. Alghamdi, “Collapsible impact energy absorbers: an overview,” *Thin-Walled Struct.*, vol. 39, no. 2, pp. 189–213, Feb. 2001.

[19] W. Abramowicz, “Thin-walled structures as impact energy absorbers,” *Thin-Walled Struct.*, vol. 41, no. 2–3, pp. 91–107, Feb. 2003.

[20] X. M. Qiu and T. X. Yu, “Some Topics in Recent Advances and Applications of Structural Impact Dynamics,” *Appl. Mech. Rev.*, vol. 64, no. 3, p. 34001, Mar. 2011.

[21] S. R. Guillow, G. Lu, and R. H. Grzebieta, “Quasi-static axial compression of thin-walled circular aluminium tubes,” *Int. J. Mech. Sci.*, vol. 43, no. 9, pp. 2103–2123, Sep. 2001.

[22] T. Wierzbicki and M. S. Suh, “Indentation of tubes under combined loading,” *Int. J.*

Mech. Sci., vol. 30, no. 3–4, pp. 229–248, Jan. 1988.

[23] Y.-Y. Jing and D. C. Barton, "The response of square cross-section tubes under lateral impact loading," *Int. J. Crashworthiness*, vol. 3, no. 4, pp. 359–378, Jun. 1998.

[24] G. Lu, "A study of the crushing of tubes by two indenters," *Int. J. Mech. Sci.*, vol. 35, no. 3–4, pp. 267–278, Mar. 1993.

[25] N. K. Gupta, G. S. Sekhon, and P. K. Gupta, "Study of lateral compression of round metallic tubes," *Thin-Walled Struct.*, vol. 43, no. 6, pp. 895–922, Jun. 2005.

[26] P. C. Miscow F. and H. A. Al-Qureshi, "Mechanics of static and dynamic inversion processes," *Int. J. Mech. Sci.*, vol. 39, no. 2, pp. 147–161, Feb. 1997.

[27] A. Niknejad and M. Moeinifard, "Theoretical and experimental studies of the external inversion process in the circular metal tubes," *Mater. Des.*, vol. 40, pp. 324–330, Sep. 2012.

[28] X. Qiu, L. He, J. Gu, and X. Yu, "A three-dimensional model of circular tube under quasi-static external free inversion," *Int. J. Mech. Sci.*, vol. 75, pp. 87–93, Oct. 2013.

[29] S. R. Reid and J. J. Harrigan, "Transient effects in the quasi-static and dynamic internal inversion and nosing of metal tubes," *Int. J. Mech. Sci.*, vol. 40, no. 2–3, pp. 263–280, Feb. 1998.

[30] X. Yu, X. Qiu, and T. X. Yu, "Analysis of the free external inversion of circular tubes based on deformation theory," *Int. J. Mech. Sci.*, vol. 100, pp. 262–268, Sep. 2015.

[31] X. Huang, G. Lu, and T. X. Yu, "On the axial splitting and curling of circular metal tubes," *Int. J. Mech. Sci.*, vol. 44, no. 11, pp. 2369–2391, Nov. 2002.

[32] X. Huang, G. Lu, and T. X. Yu, "Energy absorption in splitting square metal tubes," *Thin-Walled Struct.*, vol. 40, no. 2, pp. 153–165, Feb. 2002.

[33] W. J. Stronge, T. X. Yu, and W. Johnson, "Long stroke energy dissipation in splitting tubes," *Int. J. Mech. Sci.*, vol. 25, no. 9–10, pp. 637–647, Jan. 1983.

[34] T. Y. Reddy and S. R. Reid, “Axial splitting of circular metal tubes,” *Int. J. Mech. Sci.*, vol. 28, no. 2, pp. 111–131, Jan. 1986.

[35] P. Jiang, W. Wang, and G. J. Zhang, “Size effects in the axial tearing of circular tubes during quasi-static and impact loadings,” *Int. J. Impact Eng.*, vol. 32, no. 12, pp. 2048–2065, Dec. 2006.

[36] S. Yi Jin, W. Altenhof, and T. Kapoor, “An experimental investigation into the cutting deformation mode of AA6061-T6 round extrusions,” *Thin-Walled Struct.*, vol. 44, no. 7, pp. 773–786, Jul. 2006.

[37] M. Costas, J. Díaz, L. E. Romera, S. Hernández, and A. Tielas, “Static and dynamic axial crushing analysis of car frontal impact hybrid absorbers,” *Int. J. Impact Eng.*, vol. 62, pp. 166–181, Dec. 2013.

[38] M. Costas, D. Morin, M. Langseth, L. Romera, J. D??az, and J. Díaz, “Axial crushing of aluminum extrusions filled with PET foam and GFRP. An experimental investigation,” *Thin-Walled Struct.*, vol. 99, pp. 45–57, Feb. 2016.

[39] J. Paz, J. Díaz, L. Romera, and M. Costas, “Crushing analysis and multi-objective crashworthiness optimization of GFRP honeycomb-filled energy absorption devices,” *Finite Elem. Anal. Des.*, vol. 91, pp. 30–39, Nov. 2014.

[40] M. Costas, J. Díaz, L. Romera, and S. Hernández, “A multi-objective surrogate-based optimization of the crashworthiness of a hybrid impact absorber,” *Int. J. Mech. Sci.*, vol. 88, pp. 46–54, Nov. 2014.

[41] T. Tran, S. Hou, X. Han, W. Tan, and N. Nguyen, “Theoretical prediction and crashworthiness optimization of multi-cell triangular tubes,” *Thin-Walled Struct.*, vol. 82, pp. 183–195, Sep. 2014.

[42] T. Tran, S. Hou, X. Han, N. Nguyen, and M. Chau, “Theoretical prediction and crashworthiness optimization of multi-cell square tubes under oblique impact loading,”

Int. J. Mech. Sci., vol. 89, pp. 177–193, Dec. 2014.

[43] Z. Ahmad and D. P. Thambiratnam, "Crushing response of foam-filled conical tubes under quasi-static axial loading," *Mater. Des.*, vol. 30, no. 7, pp. 2393–2403, Aug. 2009.

[44] G. M. Nagel and D. P. Thambiratnam, "Computer simulation and energy absorption of tapered thin-walled rectangular tubes," *Thin-Walled Struct.*, vol. 43, no. 8, pp. 1225–1242, Aug. 2005.

[45] A. Baroutaji, M. D. Gilchrist, D. Smyth, and A. G. Olabi, "Analysis and optimization of sandwich tubes energy absorbers under lateral loading," *Int. J. Impact Eng.*, vol. 82, pp. 74–88, Aug. 2015.

[46] N. Qiu, Y. Gao, J. Fang, Z. Feng, G. Sun, and Q. Li, "Crashworthiness analysis and design of multi-cell hexagonal columns under multiple loading cases," *Finite Elem. Anal. Des.*, vol. 104, pp. 89–101, Oct. 2015.

[47] Y. Liu, "Crashworthiness design of multi-corner thin-walled columns," *Thin-Walled Struct.*, vol. 46, no. 12, pp. 1329–1337, Dec. 2008.

[48] R. Liang and A. S. Khan, "A critical review of experimental results and constitutive models for BCC and FCC metals over a wide range of strain rates and temperatures," *Int. J. Plast.*, vol. 15, no. 9, pp. 963–980, Jan. 1999.

[49] W. (Willem), Witteman, "Improved vehicle crashworthiness design by control of the energy absorption for different collision situations," 1999.

[50] L. Wågström, R. Thomson, and B. Pipkorn, "Structural adaptivity in frontal collisions: implications on crash pulse characteristics," *Int. J. Crashworthiness*, vol. 10, no. 4, pp. 371–378, Apr. 2005.

[51] J. M. ALEXANDER, "AN APPROXIMATE ANALYSIS OF THE COLLAPSE OF THIN CYLINDRICAL SHELLS UNDER AXIAL LOADING," *Q. J. Mech. Appl.*

Math., vol. 13, no. 1, pp. 10–15, Jan. 1960.

[52] W. Abramowicz and N. Jones, "Dynamic progressive buckling of circular and square tubes," *Int. J. Impact Eng.*, vol. 4, no. 4, pp. 243–270, Jan. 1986.

[53] W. Abramowicz and N. Jones, "Dynamic axial crushing of square tubes," *Int. J. Impact Eng.*, vol. 2, no. 2, pp. 179–208, Jan. 1984.

[54] T. Wierzbicki, S. U. Bhat, W. Abramowicz, and D. Brodkin, "Alexander revisited—A two folding elements model of progressive crushing of tubes," *Int. J. Solids Struct.*, vol. 29, no. 24, pp. 3269–3288, Jan. 1992.

[55] B. Wang and G. Lu, "Mushrooming of circular tubes under dynamic axial loading," *Thin-Walled Struct.*, vol. 40, no. 2, pp. 167–182, Feb. 2002.

[56] Z. Tang, S. Liu, and Z. Zhang, "Analysis of energy absorption characteristics of cylindrical multi-cell columns," *Thin-Walled Struct.*, vol. 62, pp. 75–84, Jan. 2013.

[57] T. Wierzbicki and W. Abramowicz, "On the Crushing Mechanics of Thin-Walled Structures," *J. Appl. Mech.*, vol. 50, no. 4a, p. 727, 1983.

[58] W. Abramowicz and N. Jones, "Transition from initial global bending to progressive buckling of tubes loaded statically and dynamically," *Int. J. Impact Eng.*, vol. 19, no. 96, pp. 415–437, May 1997.

[59] Ø. Jensen, M. Langseth, and O. S. Hopperstad, "Transition Between Progressive And Global Buckling Of Aluminium Extrusions," *WIT Trans. Built Environ.*, vol. 63, May 2002.

[60] S. S. Hsu and N. Jones, "Quasi-static and dynamic axial crushing of thin-walled circular stainless steel, mild steel and aluminium alloy tubes," *Int. J. Crashworthiness*, vol. 9, no. 2, pp. 195–217, Mar. 2004.

[61] D. Karagiozova and M. Alves, "Transition from progressive buckling to global bending of circular shells under axial impact—Part I: Experimental and numerical

observations," *Int. J. Solids Struct.*, vol. 41, no. 5–6, pp. 1565–1580, Mar. 2004.

[62] D. Karagiozova and M. Alves, "Transition from progressive buckling to global bending of circular shells under axial impact—Part II: Theoretical analysis," *Int. J. Solids Struct.*, vol. 41, no. 5, pp. 1581–1604, 2004.

[63] S. R. Reid and T. Y. Reddy, "Static and dynamic crushing of tapered sheet metal tubes of rectangular cross-section," *Int. J. Mech. Sci.*, vol. 28, no. 9, pp. 623–637, Jan. 1986.

[64] A. G. Mamalis and W. Johnson, "The quasi-static crumpling of thin-walled circular cylinders and frusta under axial compression," *Int. J. Mech. Sci.*, vol. 25, no. 9–10, pp. 713–732, Jan. 1983.

[65] A. G. Mamalis, D. E. Manolakos, S. Saigal, G. Viegelahn, and W. Johnson, "Extensible plastic collapse of thin-wall frusta as energy absorbers," *Int. J. Mech. Sci.*, vol. 28, no. 4, pp. 219–229, Jan. 1986.

[66] A. A. A. Alghamdi, "Reinversion of aluminium frustra," *Thin-Walled Struct.*, vol. 40, no. 12, pp. 1037–1049, Dec. 2002.

[67] A. A. A. Alghamdi, "Folding-crumpling of thin-walled aluminium frusta," *Int. J. Crashworthiness*, Jul. 2010.

[68] A. A. A. Alghamdi, A. A. N. Aljawi, and T. M.-N. Abu-Mansour, "Modes of axial collapse of unconstrained capped frusta," *Int. J. Mech. Sci.*, vol. 44, no. 6, pp. 1145–1161, Jun. 2002.

[69] G. M. Nagel and D. P. Thambiratnam, "Dynamic simulation and energy absorption of tapered thin-walled tubes under oblique impact loading," *Int. J. Impact Eng.*, vol. 32, no. 10, pp. 1595–1620, Oct. 2006.

[70] G. M. Nagel and D. P. Thambiratnam, "A numerical study on the impact response and energy absorption of tapered thin-walled tubes," *Int. J. Mech. Sci.*, vol. 46, no. 2, pp. 201–216, Feb. 2004.

[71] G. M. Nagel and D. P. Thambiratnam, “Dynamic simulation and energy absorption of tapered tubes under impact loading,” *Int. J. Crashworthiness*, vol. 9, no. 4, pp. 389–399, Aug. 2004.

[72] M. A. Guler, M. E. Cerit, B. Bayram, B. Gerçeker, and E. Karakaya, “The effect of geometrical parameters on the energy absorption characteristics of thin-walled structures under axial impact loading,” *Int. J. Crashworthiness*, vol. 15, no. 4, pp. 377–390, Oct. 2010.

[73] A. G. Mamalis, D. . Manolakos, M. . Ioannidis, P. . Kostazos, and C. Dimitriou, “Finite element simulation of the axial collapse of metallic thin-walled tubes with octagonal cross-section,” *Thin-Walled Struct.*, vol. 41, no. 10, pp. 891–900, Oct. 2003.

[74] A. Rossi, Z. Fawaz, and K. Behdinan, “Numerical simulation of the axial collapse of thin-walled polygonal section tubes,” *Thin-Walled Struct.*, vol. 43, no. 10, pp. 1646–1661, Oct. 2005.

[75] X. Zhang and H. Huh, “Crushing analysis of polygonal columns and angle elements,” *Int. J. Impact Eng.*, vol. 37, no. 4, pp. 441–451, Apr. 2010.

[76] W. Liu, Z. Lin, N. Wang, and X. Deng, “Dynamic performances of thin-walled tubes with star-shaped cross section under axial impact,” *Thin-Walled Struct.*, vol. 100, pp. 25–37, Mar. 2016.

[77] Y.-C. Liu and M. L. Day, “Simplified modelling of thin-walled box section beam,” *Int. J. Crashworthiness*, vol. 11, no. 3, pp. 263–272, Mar. 2006.

[78] W. Abramowicz and T. Wierzbicki, “Axial Crushing of Multicorner Sheet Metal Columns,” *J. Appl. Mech.*, vol. 56, no. 1, p. 113, 1989.

[79] A. G. Mamalis, D. E. Manolakos, A. K. Baldoukas, and G. L. Viegelahn, “Energy dissipation and associated failure modes when axially loading polygonal thin-walled cylinders,” *Thin-Walled Struct.*, vol. 12, no. 1, pp. 17–34, Jan. 1991.

[80] Z. Tang, S. Liu, and Z. Zhang, “Energy absorption properties of non-convex multi-corner thin-walled columns,” *Thin-Walled Struct.*, vol. 51, pp. 112–120, 2012.

[81] M. Yamashita, M. Gotoh, and Y. Sawairi, “Axial crush of hollow cylindrical structures with various polygonal cross-sections: Numerical simulation and experiment,” *J. Mater. Process. Technol.*, vol. 140, no. 1, pp. 59–64, 2003.

[82] Z. Fan, G. Lu, and K. Liu, “Quasi-static axial compression of thin-walled tubes with different cross-sectional shapes,” *Eng. Struct.*, vol. 55, pp. 80–89, Oct. 2013.

[83] S. Reddy, M. Abbasi, and M. Fard, “Multi-cornered thin-walled sheet metal members for enhanced crashworthiness and occupant protection,” *Thin-Walled Struct.*, vol. 94, pp. 56–66, 2015.

[84] M. Abbasi, S. Reddy, A. Ghafari-Nazari, and M. Fard, “Multiobjective crashworthiness optimization of multi-cornered thin-walled sheet metal members,” *Thin-Walled Struct.*, vol. 89, pp. 31–41, 2015.

[85] A. Alavi Nia and M. Parsapour, “Comparative analysis of energy absorption capacity of simple and multi-cell thin-walled tubes with triangular, square, hexagonal and octagonal sections,” *Thin-Walled Struct.*, vol. 74, pp. 155–165, Jan. 2014.

[86] Z. Fan, G. LU, T. X. YU, and K. LIU, “AXIAL CRUSHING OF TRIANGULAR TUBES,” *Int. J. Appl. Mech.*, vol. 5, no. 1, p. 1350008, Mar. 2013.

[87] X.-L. Zhao, D. Van Binh, R. Al-Mahaidi, and Z. Tao, “Stub column tests of fabricated square and triangular sections utilizing very high strength steel tubes,” *J. Constr. Steel Res.*, vol. 60, no. 11, pp. 1637–1661, Nov. 2004.

[88] T. Tran, “Crushing analysis under multiple impact loading cases for multi-cell triangular tubes,” *Thin Walled Struct.*, vol. 113, no. January, pp. 262–272, 2017.

[89] X. Zhang, G. Cheng, and H. Zhang, “Theoretical prediction and numerical simulation of multi-cell square thin-walled structures,” *Thin-Walled Struct.*, vol. 44, no. 11, pp.

1185–1191, 2006.

[90] J. Fang, Y. Gao, G. Sun, N. Qiu, and Q. Li, “On design of multi-cell tubes under axial and oblique impact loads,” *Thin-Walled Struct.*, vol. 95, pp. 115–126, Oct. 2015.

[91] X. Zhang and H. Zhang, “Energy absorption of multi-cell stub columns under axial compression,” *Thin-Walled Struct.*, vol. 68, pp. 156–163, Jul. 2013.

[92] W. Chen and T. Wierzbicki, “Relative merits of single-cell, multi-cell and foam-filled thin-walled structures in energy absorption,” *Thin-Walled Struct.*, vol. 39, no. 4, pp. 287–306, Apr. 2001.

[93] A. Alavi Nia and M. Parsapour, “An investigation on the energy absorption characteristics of multi-cell square tubes,” *Thin-Walled Struct.*, vol. 68, pp. 26–34, Jul. 2013.

[94] A. Najafi and M. Rais-Rohani, “Mechanics of axial plastic collapse in multi-cell, multi-corner crush tubes,” *Thin-Walled Struct.*, vol. 49, no. 1, pp. 1–12, 2011.

[95] X. Zhang and H. Zhang, “Axial crushing of circular multi-cell columns,” *Int. J. Impact Eng.*, vol. 65, pp. 110–125, Mar. 2014.

[96] S. Tabacu, “Axial crushing of circular structures with rectangular multi-cell insert,” *Thin-Walled Struct.*, vol. 95, pp. 297–309, Oct. 2015.

[97] A. Mahmoodi, M. H. Shojaeefard, and H. Saeidi Googarchin, “Theoretical development and numerical investigation on energy absorption behavior of tapered multi-cell tubes,” *Thin-Walled Struct.*, vol. 102, pp. 98–110, May 2016.

[98] X. Zhang and G. Cheng, “A comparative study of energy absorption characteristics of foam-filled and multi-cell square columns,” *Int. J. Impact Eng.*, vol. 34, no. 11, pp. 1739–1752, Nov. 2007.

[99] H. S. Kim, “New extruded multi-cell aluminum profile for maximum crash energy absorption and weight efficiency,” *Thin-Walled Struct.*, vol. 40, no. 4, pp. 311–327,

2002.

[100] X. Zhang, Z. Wen, and H. Zhang, “Axial crushing and optimal design of square tubes with graded thickness,” *Thin-Walled Struct.*, vol. 84, pp. 263–274, Nov. 2014.

[101] G. Li, Z. Zhang, G. Sun, X. Huang, and Q. Li, “Comparison of functionally-graded structures under multiple loading angles,” *Thin-Walled Struct.*, vol. 94, pp. 334–347, Sep. 2015.

[102] X. Zhang, H. Zhang, and Z. Wen, “Axial crushing of tapered circular tubes with graded thickness,” *Int. J. Mech. Sci.*, vol. 92, pp. 12–23, Mar. 2015.

[103] G. Li, F. Xu, G. Sun, and Q. Li, “A comparative study on thin-walled structures with functionally graded thickness (FGT) and tapered tubes withstanding oblique impact loading,” *Int. J. Impact Eng.*, vol. 77, no. July 2016, pp. 68–83, 2015.

[104] X. An, Y. Gao, J. Fang, G. Sun, and Q. Li, “Crashworthiness design for foam-filled thin-walled structures with functionally lateral graded thickness sheets,” *Thin-Walled Struct.*, vol. 91, pp. 63–71, Jun. 2015.

[105] A. Menouer, R. Baleh, A. Djebbar, and A. Abdul-Latif, “New generation of energy dissipating systems based on biaxial buckling,” *Thin-Walled Struct.*, vol. 85, pp. 456–465, Dec. 2014.

[106] S. Salehghaffari, M. Tajdari, M. Panahi, and F. Mokhtarnezhad, “Attempts to improve energy absorption characteristics of circular metal tubes subjected to axial loading,” *Thin-Walled Struct.*, vol. 48, no. 6, pp. 379–390, Jun. 2010.

[107] A. A. Singace and H. El-Sobky, “Behaviour of axially crushed corrugated tubes,” *Int. J. Mech. Sci.*, vol. 39, no. 3, pp. 249–268, Mar. 1997.

[108] A. Eyvazian, M. K. Habibi, A. M. Hamouda, and R. Hedayati, “Axial crushing behavior and energy absorption efficiency of corrugated tubes,” *Mater. Des.*, vol. 54, pp. 1028–1038, Feb. 2014.

[109] S. C. K. Yuen and G. N. Nurick, “The Energy-Absorbing Characteristics of Tubular Structures With Geometric and Material Modifications: An Overview,” *Appl. Mech. Rev.*, vol. 61, no. 2, p. 20802, Mar. 2008.

[110] P. H. Thornton and C. L. Magee, “The Interplay of Geometric and Materials Variables in Energy Absorption,” *J. Eng. Mater. Technol.*, vol. 99, no. 2, p. 114, Apr. 1977.

[111] N. K. Gupta and S. K. Gupta, “Effect of annealing, size and cut-outs on axial collapse behaviour of circular tubes,” *Int. J. Mech. Sci.*, vol. 35, no. 7, pp. 597–613, Jul. 1993.

[112] J. Song, Y. Chen, and G. Lu, “Light-weight thin-walled structures with patterned windows under axial crushing,” *Int. J. Mech. Sci.*, vol. 66, pp. 239–248, Jan. 2013.

[113] A. Taştan, E. Acar, M. A. Güler, and Ü. Kılınçkaya, “Optimum crashworthiness design of tapered thin-walled tubes with lateral circular cutouts,” *Thin-Walled Struct.*, vol. 107, pp. 543–553, 2016.

[114] A. Reyes, O. S. Hopperstad, and M. Langseth, “Aluminum foam-filled extrusions subjected to oblique loading: experimental and numerical study,” *Int. J. Solids Struct.*, vol. 41, no. 5–6, pp. 1645–1675, Mar. 2004.

[115] A. Reyes, M. Langseth, and O. S. Hopperstad, “Square aluminum tubes subjected to oblique loading,” *Int. J. Impact Eng.*, vol. 28, no. 10, pp. 1077–1106, Nov. 2003.

[116] A. Reyes, M. Langseth, and O. S. Hopperstad, “Crashworthiness of aluminum extrusions subjected to oblique loading: experiments and numerical analyses,” *Int. J. Mech. Sci.*, vol. 44, no. 9, pp. 1965–1984, Sep. 2002.

[117] T. Børvik, O. S. Hopperstad, a Reyes, M. Langseth, G. Solomos, and T. Dyngeland, “Empty and foam-filled circular aluminium tubes subjected to axial and oblique quasistatic loading,” *Int. J. Crashworthiness*, vol. 8, no. 5, pp. 481–494, Jan. 2003.

[118] Y. Zhang, G. Sun, X. Xu, G. Li, and Q. Li, “Multiobjective crashworthiness optimization of hollow and conical tubes for multiple load cases,” *Thin-Walled Struct.*,

vol. 82, pp. 331–342, Sep. 2014.

[119] Z. Ahmad, D. P. P. Thambiratnam, and A. C. C. C. C. Tan, “Dynamic energy absorption characteristics of foam-filled conical tubes under oblique impact loading,” *Int. J. Impact Eng.*, vol. 37, no. 5, pp. 475–488, May 2010.

[120] S. Yang and C. Qi, “Multiobjective optimization for empty and foam-filled square columns under oblique impact loading,” *Int. J. Impact Eng.*, vol. 54, pp. 177–191, Apr. 2013.

[121] C. Qi, S. Yang, and F. Dong, “Crushing analysis and multiobjective crashworthiness optimization of tapered square tubes under oblique impact loading,” *Thin-Walled Struct.*, vol. 59, pp. 103–119, Oct. 2012.

[122] J. A. DeRuntz and P. G. Hodge, “Crushing of a Tube Between Rigid Plates,” *J. Appl. Mech.*, vol. 30, no. 3, p. 391, Sep. 1963.

[123] R. G. Redwood, “Discussion: ‘Crushing of a Tube Between Rigid Plates’ (DeRuntz, Jr., John A., and Hodge, Jr., P. G., 1963, ASME J. Appl. Mech., 30, pp. 391–395),” *J. Appl. Mech.*, vol. 31, no. 2, p. 357, Jun. 1964.

[124] S. R. Reid and T. Y. Reddy, “Effect of strain hardening on the lateral compression of tubes between rigid plates,” *Int. J. Solids Struct.*, vol. 14, no. 3, pp. 213–225, Jan. 1978.

[125] T. Y. Reddy and S. R. Reid, “Phenomena associated with the crushing of metal tubes between rigid plates,” *Int. J. Solids Struct.*, vol. 16, no. 6, pp. 545–562, Jan. 1980.

[126] M. Avalle and L. Goglio, “Static lateral compression of aluminium tubes: strain gauge measurements and discussion of theoretical models,” *J. Strain Anal. Eng. Des.*, vol. 32, no. 5, pp. 335–343, Jan. 1997.

[127] S. R. Reid, “Plastic deformation mechanisms in axially compressed metal tubes used as impact energy absorbers,” *Int. J. Mech. Sci.*, vol. 35, no. 12, pp. 1035–1052, Dec.

1993.

[128] S. R. Reid and T. Y. Reddy, “Effects of strain rate on the dynamic lateral compression of tubes,” in *Proc. 2 nd Conf. Mechanical Properties of Materials at High Rates of Strain, Oxford, England, Mar. 1979,* 1980, pp. 288–298.

[129] a. Baroutaji, M. D. Gilchrist, D. Smyth, and A. G. Olabi, “Crush analysis and multi-objective optimization design for circular tube under quasi-static lateral loading,” *Thin-Walled Struct.*, vol. 86, pp. 121–131, 2015.

[130] Z. Fan, J. Shen, G. Lu, and D. Ruan, “Dynamic lateral crushing of empty and sandwich tubes,” *Int. J. Impact Eng.*, vol. 53, pp. 3–16, Mar. 2013.

[131] S. Xu, D. Ruan, G. Lu, and T. X. Yu, “Collision and rebounding of circular rings on rigid target,” *Int. J. Impact Eng.*, vol. 79, pp. 14–21, May 2015.

[132] T. Yella Reddy and S. R. Reid, “Lateral compression of tubes and tube-systems with side constraints,” *Int. J. Mech. Sci.*, vol. 21, no. 3, pp. 187–199, Jan. 1979.

[133] S. R. Reid, “Laterally compressed metal tubes as impact energy absorbers,” in *Structural Crashworthiness (eds N. Jones and T. Wierzbicki)*, 1983, p. Chapter 1.

[134] S. R. Reid, S. L. K. Drew, and J. F. Carney, “Energy absorbing capacities of braced metal tubes,” *Int. J. Mech. Sci.*, vol. 25, no. 9–10, pp. 649–667, Jan. 1983.

[135] A. Baroutaji and A.-G. Olabi, “Analysis of the Effect of the Elliptical Ratio in Tubular Energy Absorbers Under Quasi-Static Conditions,” in *Advanced Structured Materials*, vol. 16, A. Öchsner, L. F. M. da Silva, and H. Altenbach, Eds. Berlin, Heidelberg: Springer Berlin Heidelberg, 2012, pp. 323–336.

[136] L. Wu and J. F. Carney, “Initial collapse of braced elliptical tubes under lateral compression,” *Int. J. Mech. Sci.*, vol. 39, no. 9, pp. 1023–1036, Sep. 1997.

[137] L. Wu and J. F. Carney, “Experimental analyses of collapse behaviors of braced elliptical tubes under lateral compression,” *Int. J. Mech. Sci.*, vol. 40, no. 8, pp. 761–

777, Aug. 1998.

[138] N. . Gupta, G. . Sekhon, and P. . Gupta, “A study of lateral collapse of square and rectangular metallic tubes,” *Thin-Walled Struct.*, vol. 39, no. 9, pp. 745–772, Sep. 2001.

[139] A. Niknejad, S. A. M. A. Elahi, S. A. M. A. Elahi, and S. A. M. A. Elahi, “Theoretical and experimental study on the flattening deformation of the rectangular brazen and aluminum columns,” *Arch. Civ. Mech. Eng.*, vol. 13, no. 4, pp. 449–464, 2013.

[140] T. Tran and T. N. T. Ton, “Lateral crushing behaviour and theoretical prediction of thin-walled rectangular and square tubes,” *Compos. Struct.*, vol. 154, pp. 374–384, 2016.

[141] A. Niknejad and D. M. Rahmani, “Experimental and theoretical study of the lateral compression process on the empty and foam-filled hexagonal columns,” *Mater. Des.*, vol. 53, pp. 250–261, Jan. 2014.

[142] A. Baroutaji, E. Morris, and A. G. Olabi, “Quasi-static response and multi-objective crashworthiness optimization of oblong tube under lateral loading,” *Thin-Walled Struct.*, vol. 82, pp. 262–277, Sep. 2014.

[143] P. Wang, Q. Zheng, H. Fan, F. Sun, F. Jin, and Z. Qu, “Quasi-static crushing behaviors and plastic analysis of thin-walled triangular tubes,” *J. Constr. Steel Res.*, vol. 106, pp. 35–43, Mar. 2015.

[144] T. Tran, “Crushing and theoretical analysis of multi-cell thin-walled triangular tubes under lateral loading,” *Thin-Walled Struct.*, vol. 115, pp. 205–214, 2017.

[145] H. Fan, W. Hong, F. Sun, Y. Xu, and F. Jin, “Lateral compression behaviors of thin-walled equilateral triangular tubes,” *Int. J. Steel Struct.*, vol. 15, no. 4, pp. 785–795, Dec. 2015.

[146] H. Wang, J. Yang, H. Liu, Y. Sun, and T. X. X. Yu, “Internally nested circular tube

system subjected to lateral impact loading," *Thin-Walled Struct.*, vol. 91, pp. 72–81, Jun. 2015.

[147] A. Baroutaji, M. D. Gilchrist, and A. G. Olabi, "Quasi-static, impact and energy absorption of internally nested tubes subjected to lateral loading," *Thin-Walled Struct.*, vol. 98, pp. 337–350, Jan. 2016.

[148] A. G. Olabi, E. Morris, M. S. J. Hashmi, and M. D. Gilchrist, "Optimised design of nested oblong tube energy absorbers under lateral impact loading," *Int. J. Impact Eng.*, vol. 35, no. 1, pp. 10–26, Jan. 2008.

[149] E. Morris, A. G. Olabi, and M. S. J. Hashmi, "Lateral crushing of circular and non-circular tube systems under quasi-static conditions," *J. Mater. Process. Technol.*, vol. 191, no. 1–3, pp. 132–135, Aug. 2007.

[150] E. Morris, A. G. Olabi, and M. S. J. Hashmi, "Analysis of nested tube type energy absorbers with different indenters and exterior constraints," *Thin-Walled Struct.*, vol. 44, no. 8, pp. 872–885, Aug. 2006.

[151] A. G. Olabi, E. Morris, M. S. J. Hashmi, and M. D. Gilchrist, "Optimised design of nested circular tube energy absorbers under lateral impact loading," *Int. J. Mech. Sci.*, vol. 50, no. 1, pp. 104–116, 2008.

[152] Z. Wang, Z. Li, and X. Zhang, "Bending resistance of thin-walled multi-cell square tubes," *Thin-Walled Struct.*, vol. 107, pp. 287–299, 2016.

[153] T. Wierzbicki, L. Recke, W. Abramowicz, T. Gholami, and J. Huang, "Stress profiles in thin-walled prismatic columns subjected to crush loading-II. Bending," *Comput. Struct.*, vol. 51, no. 6, pp. 625–641, 1994.

[154] T. Tang, W. Zhang, H. Yin, and H. Wang, "Crushing analysis of thin-walled beams with various section geometries under lateral impact," *Thin-Walled Struct.*, vol. 102, no. May, pp. 43–57, 2016.

[155] X. Zhang, H. Zhang, and Z. Wang, “Bending collapse of square tubes with variable thickness,” *Int. J. Mech. Sci.*, vol. 106, pp. 107–116, Feb. 2016.

[156] G. Sun, X. Tian, J. Fang, F. Xu, G. Li, and X. Huang, “Dynamical bending analysis and optimization design for functionally graded thickness (FGT) tube,” *Int. J. Impact Eng.*, vol. 78, no. August, pp. 128–137, Apr. 2015.

[157] Z. Zhang, S. Liu, and Z. Tang, “Design optimization of cross-sectional configuration of rib-reinforced thin-walled beam,” *Thin-Walled Struct.*, vol. 47, no. 8–9, pp. 868–878, Aug. 2009.

[158] C. P. Gameiro and J. Cirne, “Dynamic axial crushing of short to long circular aluminium tubes with agglomerate cork filler,” *Int. J. Mech. Sci.*, vol. 49, no. 9, pp. 1029–1037, Sep. 2007.

[159] R. M. Coelho, R. J. Alves de Sousa, F. A. O. Fernandes, and F. Teixeira-Dias, “New composite liners for energy absorption purposes,” *Mater. Des.*, vol. 43, pp. 384–392, Jan. 2013.

[160] T. Y. Reddy and S. T. S. Al-Hassani, “Axial crushing of wood-filled square metal tubes,” *Int. J. Mech. Sci.*, vol. 35, no. 3–4, pp. 231–246, Mar. 1993.

[161] Z. Ahmad and D. P. Thambiratnam, “Dynamic computer simulation and energy absorption of foam-filled conical tubes under axial impact loading,” *Comput. Struct.*, vol. 87, no. 3–4, pp. 186–197, Feb. 2009.

[162] D. Tankara, R. Moradi, Y. Y. Tay, and H. M. Lankarani, “Energy Absorption Characteristics of a Thin-Walled Tube Filled With Carbon Nano Polyurethane Foam and Application in Car Bumper,” in *ASME 2014 International Mechanical Engineering Congress and Exposition*, 2014, p. V012T15A029.

[163] A. G. Hanssen, O. S. Hopperstad, and M. Langseth, “Design of aluminium foam-filled crash boxes of square and circular cross-sections,” *Int. J. Crashworthiness*, vol. 6, no.

2, pp. 177–188, Jan. 2001.

[164] A. . Markaki and T. . Clyne, “The effect of cell wall microstructure on the deformation and fracture of aluminium-based foams,” *Acta Mater.*, vol. 49, no. 9, pp. 1677–1686, May 2001.

[165] L. J. Gibson and M. F. Ashby, *Cellular Solids: Structure and Properties*. Cambridge University Press, 1999.

[166] R. Brezny and D. J. Green, “The effect of cell size on the mechanical behavior of cellular materials,” *Acta Metall. Mater.*, vol. 38, no. 12, pp. 2517–2526, Dec. 1990.

[167] C. Chen, T. J. Lu, and N. A. Fleck, “Effect of imperfections on the yielding of two-dimensional foams,” *J. Mech. Phys. Solids*, vol. 47, no. 11, pp. 2235–2272, Sep. 1999.

[168] R. Bouix, P. Viot, and J.-L. Lataillade, “Polypropylene foam behaviour under dynamic loadings: Strain rate, density and microstructure effects,” *Int. J. Impact Eng.*, vol. 36, no. 2, pp. 329–342, Feb. 2009.

[169] F. Yi, Z. Zhu, F. Zu, S. Hu, and P. Yi, “Strain rate effects on the compressive property and the energy-absorbing capacity of aluminum alloy foams,” *Mater. Charact.*, vol. 47, no. 5, pp. 417–422, Dec. 2001.

[170] H. Zhao, I. Elnasri, and S. Abdennadher, “An experimental study on the behaviour under impact loading of metallic cellular materials,” *Int. J. Mech. Sci.*, vol. 47, no. 4–5, pp. 757–774, Apr. 2005.

[171] V. L. Tagarielli, V. S. Deshpande, and N. A. Fleck, “The high strain rate response of PVC foams and end-grain balsa wood,” *Compos. Part B Eng.*, vol. 39, no. 1, pp. 83–91, Jan. 2008.

[172] P. J. Tan, S. R. Reid, J. J. Harrigan, Z. Zou, and S. Li, “Dynamic compressive strength properties of aluminium foams. Part I—experimental data and observations,” *J. Mech. Phys. Solids*, vol. 53, no. 10, pp. 2174–2205, Oct. 2005.

[173] S. Xu, D. Ruan, and G. Lu, “Strength enhancement of aluminium foams and honeycombs by entrapped air under dynamic loadings,” *Int. J. Impact Eng.*, vol. 74, pp. 120–125, Dec. 2014.

[174] S. R. Reid and C. Peng, “Dynamic uniaxial crushing of wood,” *Int. J. Impact Eng.*, vol. 19, no. 5–6, pp. 531–570, May 1997.

[175] P. J. Tan, S. R. Reid, J. J. Harrigan, Z. Zou, and S. Li, “Dynamic compressive strength properties of aluminium foams. Part II—‘shock’ theory and comparison with experimental data and numerical models,” *J. Mech. Phys. Solids*, vol. 53, no. 10, pp. 2206–2230, Oct. 2005.

[176] S. R. Reid, T. Y. Reddy, and C. Peng, “Dynamic compression of cellular structures and materials,” in *In: Jones, N., Wierzbicki, T. (Eds.), Structural Crashworthiness and Failure, Elsevier Applied Science Publishers*, 1993, pp. 295–340.

[177] A. G. Hanssen, O. S. Hopperstad, M. Langseth, and H. Ilstad, “Validation of constitutive models applicable to aluminium foams,” *Int. J. Mech. Sci.*, vol. 44, no. 2, pp. 359–406, 2002.

[178] H. Fang, J. Bi, C. Zhang, M. Gutowski, E. Palta, and Q. Wang, “A constitutive model of aluminum foam for crash simulations,” *Int. J. Non. Linear. Mech.*, vol. 90, pp. 124–136, 2017.

[179] S. Gaitanaros and S. Kyriakides, “On the effect of relative density on the crushing and energy absorption of open-cell foams under impact,” *Int. J. Impact Eng.*, vol. 82, pp. 3–13, Aug. 2015.

[180] S. R. Reid and T. Y. Reddy, “Axial crushing of foam-filled tapered sheet metal tubes,” *Int. J. Mech. Sci.*, vol. 28, no. 10, pp. 643–656, Jan. 1986.

[181] S. R. Reid, T. Y. Reddy, and M. D. Gray, “Static and dynamic axial crushing of foam-filled sheet metal tubes,” *Int. J. Mech. Sci.*, vol. 28, no. 5, pp. 295–322, Jan. 1986.

[182] A. G. Hanssen, M. Langseth, and O. S. Hopperstad, “Static and dynamic crushing of circular aluminium extrusions with aluminium foam filler,” *Int. J. Impact Eng.*, vol. 24, no. 5, pp. 475–507, Apr. 2000.

[183] S. P. Santosa, T. Wierzbicki, A. G. Hanssen, and M. Langseth, “Experimental and numerical studies of foam-filled sections,” *Int. J. Impact Eng.*, vol. 24, no. 5, pp. 509–534, May 2000.

[184] M. Seitzberger, F. G. Rammerstorfer, R. Gradinger, H. P. Degischer, M. Blaimschein, and C. Walch, “Experimental studies on the quasi-static axial crushing of steel columns filled with aluminium foam,” *Int. J. Solids Struct.*, vol. 37, no. 30, pp. 4125–4147, Jul. 2000.

[185] H. R. Zarei and M. Kröger, “Optimization of the foam-filled aluminum tubes for crush box application,” *Thin-Walled Struct.*, vol. 46, no. 2, pp. 214–221, Feb. 2008.

[186] H. Kavi, A. K. Toksoy, and M. Guden, “Predicting energy absorption in a foam-filled thin-walled aluminum tube based on experimentally determined strengthening coefficient,” *Mater. Des.*, vol. 27, no. 4, pp. 263–269, Jan. 2006.

[187] A. K. Toksoy and M. Güden, “The strengthening effect of polystyrene foam filling in aluminum thin-walled cylindrical tubes,” *Thin-Walled Struct.*, vol. 43, no. 2, pp. 333–350, Feb. 2005.

[188] W. Yan, E. Durif, Y. Yamada, and C. Wen, “Crushing Simulation of Foam-Filled Aluminium Tubes,” *Mater. Trans.*, vol. 48, no. 7, pp. 1901–1906, Jun. 2007.

[189] L. Mirfendereski, M. Salimi, and S. Ziaei-Rad, “Parametric study and numerical analysis of empty and foam-filled thin-walled tubes under static and dynamic loadings,” *Int. J. Mech. Sci.*, vol. 50, no. 6, pp. 1042–1057, Jun. 2008.

[190] W. Chen, “Experimental and numerical study on bending collapse of aluminum foam-filled hat profiles,” *Int. J. Solids Struct.*, vol. 38, no. 44–45, pp. 7919–7944, Nov.

2001.

[191] H.-W. Song, Z.-J. Fan, G. Yu, Q.-C. Wang, and A. Tobota, “Partition energy absorption of axially crushed aluminum foam-filled hat sections,” *Int. J. Solids Struct.*, vol. 42, no. 9–10, pp. 2575–2600, May 2005.

[192] W. Altenhof, A.-M. Harte, and R. Turchi, “Experimental and numerical compressive testing of aluminum foam filled mild steel tubular hat sections,” in *7th International LS-DYNA Users Conference*, 2002, no. 3, pp. 19–28.

[193] A. Reyes, O. S. Hopperstad, A. G. Hanssen, and M. Langseth, “Modeling of material failure in foam-based components,” *Int. J. Impact Eng.*, vol. 30, no. 7, pp. 805–834, Aug. 2004.

[194] J. Banhart, “Manufacture, characterisation and application of cellular metals and metal foams,” *Prog. Mater. Sci.*, vol. 46, no. 6, pp. 559–632, Jan. 2001.

[195] A. G. Hanssen, M. Langseth, and O. S. Hopperstad, “Optimum design for energy absorption of square aluminium columns with aluminium foam filler,” *Int. J. Mech. Sci.*, vol. 43, no. 1, pp. 153–176, Jan. 2001.

[196] S. Asavavisithchai, D. Slater, and A. R. Kennedy, “Effect of tube length on the bucking mode and energy absorption of Al foam-filled tubes,” *J. Mater. Sci.*, vol. 39, no. 24, pp. 7395–7396, Dec. 2004.

[197] N. Onsalung, C. Thinvongpituk, and K. Painthong, “The Influence of Foam Density on Specific Energy Absorption of Rectangular Steel Tubes,” *Energy Res. J.*, vol. 1, no. 2, pp. 135–140, 2010.

[198] M. Seitzberger, F. G. Rammerstorfer, H. P. Degischer, and R. Gradinger, “Crushing of axially compressed steel tubes filled with aluminium foam,” *Acta Mech.*, vol. 125, no. 1–4, pp. 93–105, Mar. 1997.

[199] S. Santosa and T. Wierzbicki, “Crash behavior of box columns filled with aluminum

honeycomb or foam," *Comput. Struct.*, vol. 68, no. 4, pp. 343–367, 1998.

[200] P. H. Thornton, "Energy Absorption by Foam Filled Structures," in *SAE Technical Paper 800081*, 1980.

[201] P. H. Thornton, H. F. Mahmood, and C. L. Magee, "Energy absorption by structural collapse," in *Chapter4 in Structural Crashworthiness (eds N. Jones and T. Wierzbicki), Butterworths, London*, 1983, pp. 96–117.

[202] Q. Gao, L. Wang, Y. Wang, and C. Wang, "Crushing analysis and multiobjective crashworthiness optimization of foam-filled ellipse tubes under oblique impact loading," *Thin-Walled Struct.*, vol. 100, pp. 105–112, Mar. 2016.

[203] Q. Gao, L. Wang, Y. Wang, F. Guo, and Z. Zhang, "Optimization of foam-filled double ellipse tubes under multiple loading cases," *Adv. Eng. Softw.*, vol. 99, pp. 27–35, 2016.

[204] S. Shahbeyk, A. Vafai, and N. Petrinic, "Axial crushing of metal foam-filled square columns: Foam density distribution and impactor inclination effects," *Thin-Walled Struct.*, vol. 43, no. 12, pp. 1818–1830, Dec. 2005.

[205] J. Shen, G. Lu, D. Ruan, and C. Chiang Seah, "Lateral plastic collapse of sandwich tubes with metal foam core," *Int. J. Mech. Sci.*, vol. 91, pp. 99–109, Feb. 2015.

[206] A. Baroutaji and A. G. Olabi, "Lateral collapse of short-length sandwich tubes compressed by different indenters and exposed to external constraints," *Materwiss. Werksttech.*, vol. 45, no. 5, p. n/a-n/a, May 2014.

[207] A. Niknejad, S. A. Elahi, and G. H. Liaghat, "Experimental investigation on the lateral compression in the foam-filled circular tubes," *Mater. Des.*, vol. 36, pp. 24–34, Apr. 2012.

[208] Z. Fan, J. Shen, and G. Lu, "Investigation of lateral crushing of sandwich tubes," *Procedia Eng.*, vol. 14, pp. 442–449, 2011.

[209] A. Niknejad and P. H. H. Orojloo, “A novel nested system of tubes with special cross-section as the energy absorber,” *Thin-Walled Struct.*, vol. 100, pp. 113–123, Mar. 2016.

[210] H. R. Zarei and M. Kröger, “Bending behavior of empty and foam-filled beams: Structural optimization,” *Int. J. Impact Eng.*, vol. 35, no. 6, pp. 521–529, Jun. 2008.

[211] S. Santosa and T. Wierzbicki, “Effect of an ultralight metal filler on the bending collapse behavior of thin-walled prismatic columns,” *Int. J. Mech. Sci.*, vol. 41, no. 8, pp. 995–1019, Aug. 1999.

[212] Z. Li, Z. Zheng, J. Yu, and L. Guo, “Crashworthiness of foam-filled thin-walled circular tubes under dynamic bending,” *Mater. Des.*, vol. 52, pp. 1058–1064, Dec. 2013.

[213] I. Duarte, M. Vesenjak, and L. Krstulovic-Opara, “Dynamic and quasi-static bending behaviour of thin-walled aluminium tubes filled with aluminium foam,” *Compos. Struct.*, vol. 109, no. 1, pp. 48–56, 2014.

[214] B. Kieback, A. Neubrand, and H. Riedel, “Processing techniques for functionally graded materials,” *Mater. Sci. Eng. A*, vol. 362, no. 1–2, pp. 81–106, Dec. 2003.

[215] Y. Matsumoto, A. H. Brothers, S. R. Stock, and D. C. Dunand, “Uniform and graded chemical milling of aluminum foams,” *Mater. Sci. Eng. A*, vol. 447, no. 1–2, pp. 150–157, Feb. 2007.

[216] A. H. Brothers and D. C. Dunand, “Mechanical properties of a density-graded replicated aluminum foam,” *Mater. Sci. Eng. A*, vol. 489, no. 1–2, pp. 439–443, Aug. 2008.

[217] N. Gupta, “A functionally graded syntactic foam material for high energy absorption under compression,” *Mater. Lett.*, vol. 61, no. 4–5, pp. 979–982, Feb. 2007.

[218] N. Gupta and W. Ricci, “Comparison of compressive properties of layered syntactic

foams having gradient in microballoon volume fraction and wall thickness," *Mater. Sci. Eng. A*, vol. 427, no. 1–2, pp. 331–342, Jul. 2006.

[219] L. Cui, S. Kiernan, and M. D. Gilchrist, "Designing the energy absorption capacity of functionally graded foam materials," *Mater. Sci. Eng. A*, vol. 507, no. 1–2, pp. 215–225, May 2009.

[220] H. Yin, G. Wen, X. Wu, Q. Qing, and S. Hou, "Crashworthiness design of functionally graded foam-filled multi-cell thin-walled structures," *Thin-Walled Struct.*, vol. 85, pp. 142–155, Dec. 2014.

[221] G. Sun, G. Li, S. Hou, S. Zhou, W. Li, and Q. Li, "Crashworthiness design for functionally graded foam-filled thin-walled structures," *Mater. Sci. Eng. A*, vol. 527, no. 7–8, pp. 1911–1919, Mar. 2010.

[222] H. Yin, G. Wen, H. Fang, Q. Qing, X. Kong, J. Xiao, and Z. Liu, "Multiobjective crashworthiness optimization design of functionally graded foam-filled tapered tube based on dynamic ensemble metamodel," *Mater. Des.*, vol. 55, pp. 747–757, Mar. 2014.

[223] Y. zhang, M. Lu, G. Sun, G. Li, and Q. Li, "On functionally graded composite structures for crashworthiness," *Compos. Struct.*, vol. 132, pp. 393–405, Nov. 2015.

[224] M. S. Attia, S. A. Meguid, and H. Nouraei, "Nonlinear finite element analysis of the crush behaviour of functionally graded foam-filled columns," *Finite Elem. Anal. Des.*, vol. 61, pp. 50–59, Nov. 2012.

[225] J. Fang, Y. Gao, X. An, G. Sun, J. Chen, and Q. Li, "Design of transversely-graded foam and wall thickness structures for crashworthiness criteria," *Compos. Part B Eng.*, vol. 92, pp. 338–349, May 2016.

[226] R. D. Hussein, D. Ruan, G. Lu, S. Guillow, and J. W. Yoon, "Crushing response of square aluminium tubes filled with polyurethane foam and aluminium honeycomb,"

Thin-Walled Struct., vol. 110, no. June 2016, pp. 140–154, 2017.

[227] H. Yin, G. Wen, S. Hou, and K. Chen, "Crushing analysis and multiobjective crashworthiness optimization of honeycomb-filled single and bitubular polygonal tubes," *Mater. Des.*, vol. 32, no. 8–9, pp. 4449–4460, 2011.

[228] G. Zhu, S. Li, G. Sun, G. Li, and Q. Li, "On design of graded honeycomb filler and tubal wall thickness for multiple load cases," *Thin-Walled Struct.*, vol. 109, pp. 377–389, 2016.

[229] S. Mohsenizadeh, R. Alipour, M. Shokri Rad, A. Farokhi Nejad, and Z. Ahmad, "Crashworthiness assessment of auxetic foam-filled tube under quasi-static axial loading," *Mater. Des.*, vol. 88, pp. 258–268, Dec. 2015.

[230] J. Marzbanrad and M. R. Ebrahimi, "Multi-Objective Optimization of aluminum hollow tubes for vehicle crash energy absorption using a genetic algorithm and neural networks," *Thin-Walled Struct.*, vol. 49, no. 12, pp. 1605–1615, 2011.

[231] M. Shakeri, R. Mirzaeifar, and S. Salehghaffari, "New insights into the collapsing of cylindrical thin-walled tubes under axial impact load," *Proc. Inst. Mech. Eng. Part C-Journal Mech. Eng. Sci.*, vol. 221, no. 8, pp. 869–885, 2007.

[232] L. Shi, P. Zhu, R.-J. Yang, and S.-P. Lin, "Adaptive sampling-based RBDO method for vehicle crashworthiness design using Bayesian metric and stochastic sensitivity analysis with independent random variables," *Int. J. Crashworthiness*, vol. 18, no. 4, pp. 331–342, Aug. 2013.

[233] L. Shi, R.-J. Yang, and P. Zhu, "An adaptive response surface method for crashworthiness optimization," *Eng. Optim.*, vol. 45, no. 11, pp. 1365–1377, Nov. 2013.

[234] J. Fang, G. Sun, N. Qiu, N. H. Kim, and Q. Li, "On design optimization for structural crashworthiness and its state of the art," *Struct. Multidiscip. Optim.*, no. January, 2016.

[235] H. R. Zarei and M. Kroger, “Optimum honeycomb filled crash absorber design,” *Mater. Des.*, vol. 29, no. 1, pp. 193–204, 2008.

[236] X. Zhang, G. Cheng, B. Wang, and H. Zhang, “Optimum design for energy absorption of bitubal hexagonal columns with honeycomb core,” *Int. J. Crashworthiness*, vol. 13, no. 1, pp. 99–107, Jan. 2008.

[237] M. Abbasi, R. Kazemi, and A. Ghafari Nazari, “Using a Parametric Method for Investigating Automotive Crashworthiness,” *Int. J. Automot. Eng.*, vol. 1, no. 3, pp. 165–172, 2011.

[238] S. Salehghaffari, M. Rais-Rohani, and A. Najafi, “Analysis and optimization of externally stiffened crush tubes,” *Thin-Walled Struct.*, vol. 49, no. 3, pp. 397–408, Mar. 2011.

[239] M. Abbasi, A. Ghafari-Nazari, S. Reddy, and M. Fard, “A new approach for optimizing automotive crashworthiness: concurrent usage of ANFIS and Taguchi method,” *Struct. Multidiscip. Optim.*, vol. 49, no. 3, pp. 485–499, Mar. 2014.

[240] E. Acar, M. A. Guler, B. Gereker, M. E. Cerit, and B. Bayram, “Multi-objective crashworthiness optimization of tapered thin-walled tubes with axisymmetric indentations,” *Thin-Walled Struct.*, vol. 49, no. 1, pp. 94–105, 2011.

[241] J. Fang, Y. Gao, G. Sun, N. Qiu, and Q. Li, “On design of multi-cell tubes under axial and oblique impact loads,” *Thin-Walled Struct.*, vol. 95, pp. 115–126, Oct. 2015.

[242] F. Xu, “Enhancing material efficiency of energy absorbers through graded thickness structures,” *Thin-Walled Struct.*, vol. 97, pp. 250–265, Dec. 2015.

[243] G. Sun, F. Xu, G. Li, and Q. Li, “Crashing analysis and multiobjective optimization for thin-walled structures with functionally graded thickness,” *Int. J. Impact Eng.*, vol. 64, pp. 62–74, Feb. 2014.

[244] Q. Gao, L. Wang, Y. Wang, and C. Wang, “Crushing analysis and multiobjective

crashworthiness optimization of foam-filled ellipse tubes under oblique impact loading," *Thin-Walled Struct.*, vol. 100, pp. 105–112, Mar. 2016.

[245] Y. Zhang, G. Sun, G. Li, Z. Luo, and Q. Li, "Optimization of foam-filled bitubal structures for crashworthiness criteria," *Mater. Des.*, vol. 38, pp. 99–109, Jun. 2012.

[246] S. Hou, Q. Li, S. Long, X. Yang, and W. Li, "Multiobjective optimization of multi-cell sections for the crashworthiness design," *Int. J. Impact Eng.*, vol. 35, no. 11, pp. 1355–1367, Nov. 2008.

[247] X. Gu, G. Sun, G. Li, L. Mao, and Q. Li, "A Comparative study on multiobjective reliable and robust optimization for crashworthiness design of vehicle structure," *Struct. Multidiscip. Optim.*, vol. 48, no. 3, pp. 669–684, Apr. 2013.

[248] G. Sun, X. Song, S. Baek, and Q. Li, "Robust optimization of foam-filled thin-walled structure based on sequential Kriging metamodel," *Struct. Multidiscip. Optim.*, vol. 49, no. 6, pp. 897–913, 2014.

[249] J. Fang, Y. Gao, G. Sun, Y. Zhang, and Q. Li, "Crashworthiness design of foam-filled bitubal structures with uncertainty," *Int. J. Non. Linear. Mech.*, vol. 67, pp. 120–132, Dec. 2014.

[250] J. Fang, Y. Gao, G. Sun, and Q. Li, "Multiobjective reliability-based optimization for design of a vehicledoor," *Finite Elem. Anal. Des.*, vol. 67, pp. 13–21, May 2013.

[251] Z. Xiao, J. Fang, G. Sun, and Q. Li, "Crashworthiness design for functionally graded foam-filled bumper beam," *Adv. Eng. Softw.*, vol. 85, no. 7–8, pp. 81–95, Jul. 2015.

[252] F. Pan and P. Zhu, "Design optimisation of vehicle roof structures: benefits of using multiple surrogates," *Int. J. Crashworthiness*, vol. 16, no. 1, pp. 85–95, Apr. 2011.

[253] P. Zhu, Y. Zhang, and G. Chen, "Metamodeling development for reliability-based design optimization of automotive body structure," *Comput. Ind.*, vol. 62, no. 7, pp. 729–741, Sep. 2011.

[254] H. Fang, M. Rais-Rohani, Z. Liu, and M. F. Horstemeyer, “A comparative study of metamodeling methods for multiobjective crashworthiness optimization,” *Comput. Struct.*, vol. 83, no. 25–26, pp. 2121–2136, Sep. 2005.

[255] S. Hou, D. Dong, L. Ren, and X. Han, “Multivariable crashworthiness optimization of vehicle body by unreplicated saturated factorial design,” *Struct. Multidiscip. Optim.*, vol. 46, no. 6, pp. 891–905, May 2012.

[256] X. Liao, Q. Li, X. Yang, W. Zhang, and W. Li, “Multiobjective optimization for crash safety design of vehicles using stepwise regression model,” *Struct. Multidiscip. Optim.*, vol. 35, no. 6, pp. 561–569, Nov. 2007.

[257] A. R. Yildiz and K. N. Solanki, “Multi-objective optimization of vehicle crashworthiness using a new particle swarm based approach,” *Int. J. Adv. Manuf. Technol.*, vol. 59, no. 1–4, pp. 367–376, Sep. 2011.

[258] X. Gu, G. Sun, G. Li, X. Huang, Y. Li, and Q. Li, “Multiobjective optimization design for vehicle occupant restraint system under frontal impact,” *Struct. Multidiscip. Optim.*, vol. 47, no. 3, pp. 465–477, May 2013.

[259] S. Hou, T. Liu, D. Dong, and X. Han, “Factor screening and multivariable crashworthiness optimization for vehicle side impact by factorial design,” *Struct. Multidiscip. Optim.*, vol. 49, no. 1, pp. 147–167, Oct. 2013.

[260] P. Xu, C. Yang, Y. Peng, S. Yao, D. Zhang, and B. Li, “Crash performance and multi-objective optimization of a gradual energy-absorbing structure for subway vehicles,” *Int. J. Mech. Sci.*, Jan. 2016.

[261] J. Li, G. Gao, and H. Dong, “Crushing analysis and multi-objective optimization of a railway vehicle driver’s cab,” *Thin-Walled Struct.*, vol. 107, pp. 554–563, 2016.

[262] A. Baroutaji, “Energy absorption through the lateral collapse of thin-walled single and nested tubes,” *Baroutaji, Ahmad Energy Absorpt. through lateral collapse thin-walled*

single nested tubes. PhD thesis, Dublin City Univ., 2014.

[263] I. . Mcgregor, "Impact performance of aluminium structures," in *Structural Crashworthiness (eds N. Jones and T. Wierzbicki)*, 1983, pp. 385–421.

[264] Y. Chen, A. H. Clausen, O. S. Hopperstad, and M. Langseth, "Stress–strain behaviour of aluminium alloys at a wide range of strain rates," *Int. J. Solids Struct.*, vol. 46, no. 21, pp. 3825–3835, Oct. 2009.

[265] L. Djapic Oosterkamp, A. Ivankovic, and G. Venizelos, "High strain rate properties of selected aluminium alloys," *Mater. Sci. Eng. A*, vol. 278, no. 1–2, pp. 225–235, Feb. 2000.

[266] A. Reyes, O. S. Hopperstad, O.-G. Lademo, and M. Langseth, "Modeling of textured aluminum alloys used in a bumper system: Material tests and characterization," *Comput. Mater. Sci.*, vol. 37, no. 3, pp. 246–268, Sep. 2006.

[267] T. Børvik, A. H. Clausen, M. Eriksson, T. Berstad, O. Sture Hopperstad, and M. Langseth, "Experimental and numerical study on the perforation of AA6005-T6 panels," *Int. J. Impact Eng.*, vol. 32, no. 1–4, pp. 35–64, Dec. 2005.

[268] R. Smerd, S. Winkler, C. Salisbury, M. Worswick, D. Lloyd, and M. Finn, "High strain rate tensile testing of automotive aluminum alloy sheet," *Int. J. Impact Eng.*, vol. 32, no. 1–4, pp. 541–560, Dec. 2005.

[269] E. Cadoni, L. Fenu, and D. Forni, "Strain rate behaviour in tension of austenitic stainless steel used for reinforcing bars," *Constr. Build. Mater.*, vol. 35, pp. 399–407, Oct. 2012.

[270] M. Itabashi and K. Kawata, "Carbon content effect on high-strain-rate tensile properties for carbon steels," *Int. J. Impact Eng.*, vol. 24, no. 2, pp. 117–131, Feb. 2000.

[271] E. El-Magd and M. Abouridouane, "Characterization, modelling and simulation of

deformation and fracture behaviour of the light-weight wrought alloys under high strain rate loading," *Int. J. Impact Eng.*, vol. 32, no. 5, pp. 741–758, May 2006.

[272] A. A. Nia, J. H. Hamedani, A. Alavi Nia, and J. Haddad Hamedani, "Comparative analysis of energy absorption and deformations of thin walled tubes with various section geometries," *Thin-Walled Struct.*, vol. 48, no. 12, pp. 946–954, Dec. 2010.

[273] F. Tarlochan, F. Samer, A. M. S. Hamouda, S. Ramesh, and K. Khalid, "Design of thin wall structures for energy absorption applications: Enhancement of crashworthiness due to axial and oblique impact forces," *Thin-Walled Struct.*, vol. 71, pp. 7–17, Oct. 2013.

[274] S. Pirmohammad and S. E. Marzdashti, "Crushing behavior of new designed multi-cell members subjected to axial and oblique quasi-static loads," *Thin-Walled Struct.*, vol. 108, pp. 291–304, 2016.

[275] N. Jones and W. Abramowicz, "Static and dynamic axial crushing of circular and square tubes," *Reid SR, Ed. Met. Form. impact Mech.*, vol. 47, p. 225, 1985.

[276] A. A. Singace, "Axial crushing analysis of tubes deforming in the multi-lobe mode," *Int. J. Mech. Sci.*, vol. 41, no. 7, pp. 865–890, Jul. 1999.

[277] S. Ouellet, D. Cronin, and M. Worswick, "Compressive response of polymeric foams under quasi-static, medium and high strain rate conditions," *Polym. Test.*, vol. 25, no. 6, pp. 731–743, Sep. 2006.

[278] W. Chen, F. Lu, and N. Winfree, "High-strain-rate compressive behavior of a rigid polyurethane foam with various densities," *Exp. Mech.*, vol. 42, no. 1, pp. 65–73, Mar. 2002.

[279] V. S. Deshpande and N. A. Fleck, "High strain rate compressive behaviour of aluminium alloy foams," *Int. J. Impact Eng.*, vol. 24, no. 3, pp. 277–298, Mar. 2000.

[280] K. A. Dannemann and J. Lankford, "High strain rate compression of closed-cell

aluminium foams," *Mater. Sci. Eng. A*, vol. 293, no. 1–2, pp. 157–164, Nov. 2000.

[281] S. Kiernan, L. Cui, and M. D. Gilchrist, "Propagation of a stress wave through a virtual functionally graded foam," *Int. J. Non. Linear. Mech.*, vol. 44, no. 5, pp. 456–468, Jun. 2009.

[282] A. G. Hanssen, M. Langseth, and O. S. Hopperstad, "Static and dynamic crushing of square aluminium extrusions with aluminium foam filler," *Int. J. Impact Eng.*, vol. 24, no. 4, pp. 347–383, 2000.

[283] Y. Liu, "Optimum design of straight thin-walled box section beams for crashworthiness analysis," *Finite Elem. Anal. Des.*, vol. 44, no. 3, pp. 139–147, Jan. 2008.

[284] T. Tran, S. Hou, X. Han, and M. Chau, "Crushing analysis and numerical optimization of angle element structures under axial impact loading," *Compos. Struct.*, vol. 119, pp. 422–435, Jan. 2015.

[285] S. Wu, G. Zheng, G. Sun, Q. Liu, G. Li, and Q. Li, "On design of multi-cell thin-wall structures for crashworthiness," *Int. J. Impact Eng.*, vol. 88, pp. 102–117, Feb. 2016.

[286] J. Fang, Y. Gao, G. Sun, G. Zheng, and Q. Li, "Dynamic crashing behavior of new extrudable multi-cell tubes with a functionally graded thickness," *Int. J. Mech. Sci.*, vol. 103, pp. 63–73, Nov. 2015.

[287] G. Sun, T. Pang, J. Fang, G. Li, and Q. Li, "Parameterization of criss-cross configurations for multiobjective crashworthiness optimization," *Int. J. Mech. Sci.*, vol. 124, no. January, pp. 145–157, 2017.

[288] A. Asanjarani, S. H. Dibajian, and A. Mahdian, "Multi-objective crashworthiness optimization of tapered thin-walled square tubes with indentations," *Thin-Walled Struct.*, vol. 116, pp. 26–36, 2017.

[289] S. Hou, Q. Li, S. Long, X. Yang, and W. Li, "Design optimization of regular

hexagonal thin-walled columns with crashworthiness criteria," *Finite Elem. Anal. Des.*, vol. 43, no. 6–7, pp. 555–565, Apr. 2007.

[290] H. R. Zarei and M. Kröger, "Multiobjective crashworthiness optimization of circular aluminum tubes," *Thin-Walled Struct.*, vol. 44, no. 3, pp. 301–308, Mar. 2006.

[291] S. Wu, G. Li, G. Sun, X. Wu, and Q. Li, "Crashworthiness analysis and optimization of sinusoidal corrugation tube," *Thin-Walled Struct.*, vol. 105, no. August, pp. 121–134, Aug. 2016.

[292] H. Zhang and X. Zhang, "Crashworthiness performance of conical tubes with nonlinear thickness distribution," *Thin-Walled Struct.*, vol. 99, pp. 35–44, Feb. 2016.

[293] E. Acar, M. A. Guler, B. Gerçeker, M. E. Cerit, and B. Bayram, "Multi-objective crashworthiness optimization of tapered thin-walled tubes with axisymmetric indentations," *Thin-Walled Struct.*, vol. 49, no. 1, pp. 94–105, Jan. 2011.

[294] S. Hou, Q. Li, S. Long, X. Yang, and W. Li, "Crashworthiness design for foam filled thin-wall structures," *Mater. Des.*, vol. 30, no. 6, pp. 2024–2032, Jun. 2009.

[295] H. Yin, G. Wen, S. Hou, and Q. Qing, "Multiobjective crashworthiness optimization of functionally lateral graded foam-filled tubes," *Mater. Des.*, vol. 44, pp. 414–428, Feb. 2013.

[296] H. Yin, G. Wen, Z. Liu, and Q. Qing, "Crashworthiness optimization design for foam-filled multi-cell thin-walled structures," *Thin-Walled Struct.*, vol. 75, pp. 8–17, Feb. 2014.

[297] X. Song, G. Sun, G. Li, W. Gao, and Q. Li, "Crashworthiness optimization of foam-filled tapered thin-walled structure using multiple surrogate models," *Struct. Multidiscip. Optim.*, vol. 47, no. 2, pp. 221–231, Jul. 2012.

[298] G. Zheng, S. Wu, G. Sun, G. Li, and Q. Li, "Crushing analysis of foam-filled single and bitubal polygonal thin-walled tubes," *Int. J. Mech. Sci.*, vol. 87, pp. 226–240,

2014.

[299] Y. Chen, Z. Bai, L. Zhang, Y. Wang, G. Sun, and L. Cao, “Crashworthiness analysis of octagonal multi-cell tube with functionally graded thickness under multiple loading angles,” *Thin-Walled Struct.*, vol. 110, no. July 2016, pp. 133–139, 2017.

[300] J. Fang, Y. Gao, G. Sun, Y. Zhang, and Q. Li, “Parametric analysis and multiobjective optimization for functionally graded foam-filled thin-wall tube under lateral impact,” *Comput. Mater. Sci.*, vol. 90, pp. 265–275, Jul. 2014.

[301] H. Yin, Y. Xiao, G. Wen, Q. Qing, and Y. Deng, “Multiobjective optimization for foam-filled multi-cell thin-walled structures under lateral impact,” *Thin-Walled Struct.*, vol. 94, pp. 1–12, Sep. 2015.

[302] H. Yin, Y. Xiao, G. Wen, Q. Qing, and X. Wu, “Crushing analysis and multi-objective optimization design for bionic thin-walled structure,” *Mater. Des.*, vol. 87, pp. 825–834, Dec. 2015.

Figure 1: Most common loading/deformation modes of TW tubes used in automobiles

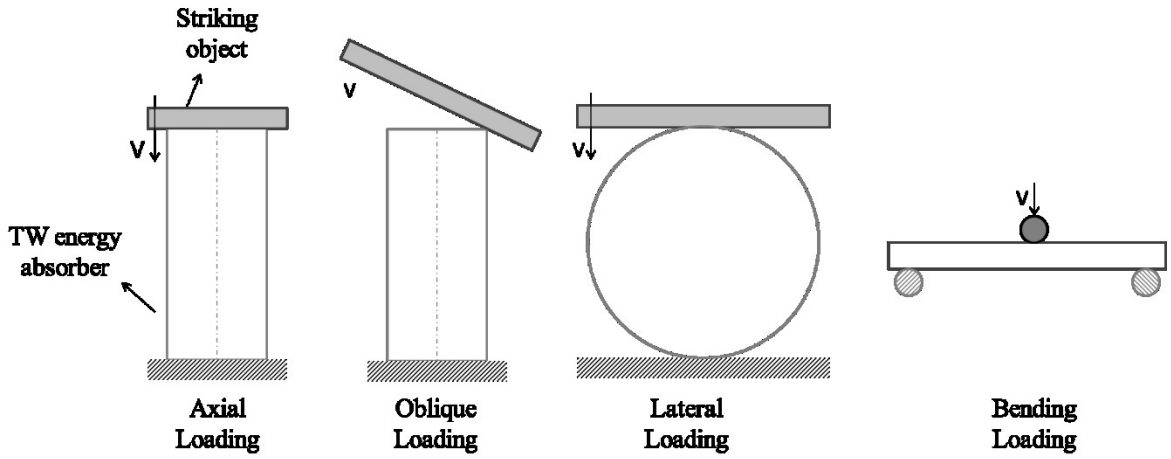

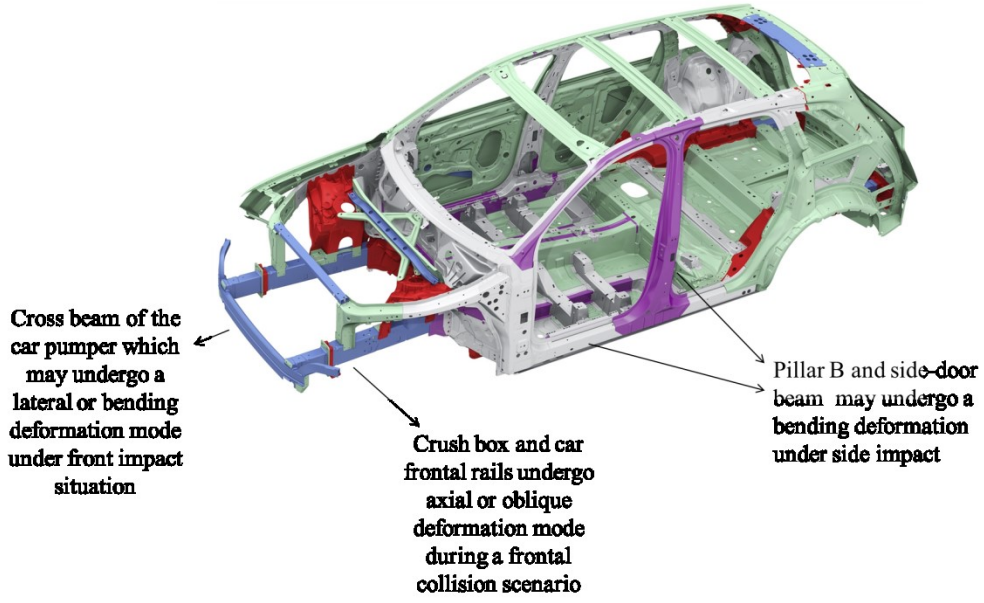

Figure 2: Various deformation modes of axially loaded circular tubes: (a) axisymmetric mode; (b) non-symmetric mode; and (c) mixed deformation mode [21].

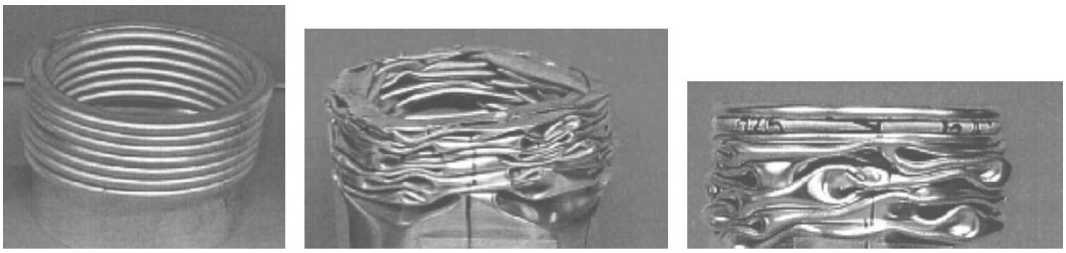

(a) (b) (c)

Figure 3: Mild steel samples: Deformation states at velocities of 385 m/s, 277 m/s, 227 m/s, 173m/s and 0 m/s respectively [55].

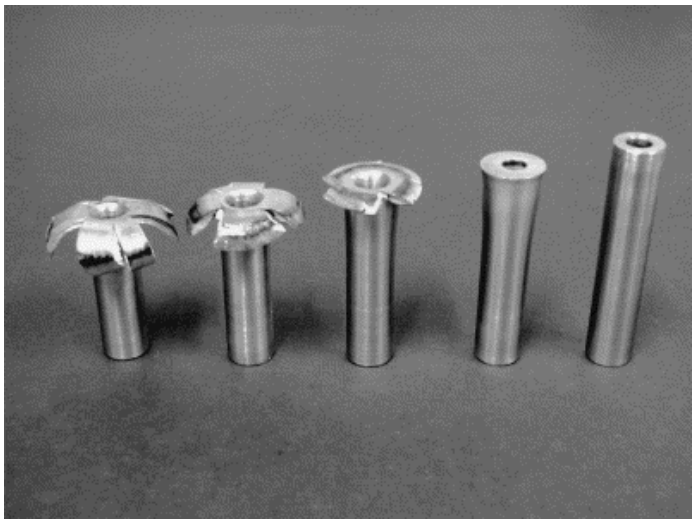

Figure 4: Axial progressive deformation modes of square tubes: (a) extensional mode develops in tubes with b/t <7.5 (b) inextenstional mode occurs in tubes with approximately $b/t > 40.8$, (c) asymmetric mixed-mode occurs in tubes with $7.5 \leq b/t \leq 40.8$ [2], (d) non-compact crushing mode occurs in very thin tube $b/t \approx 100$ [127]

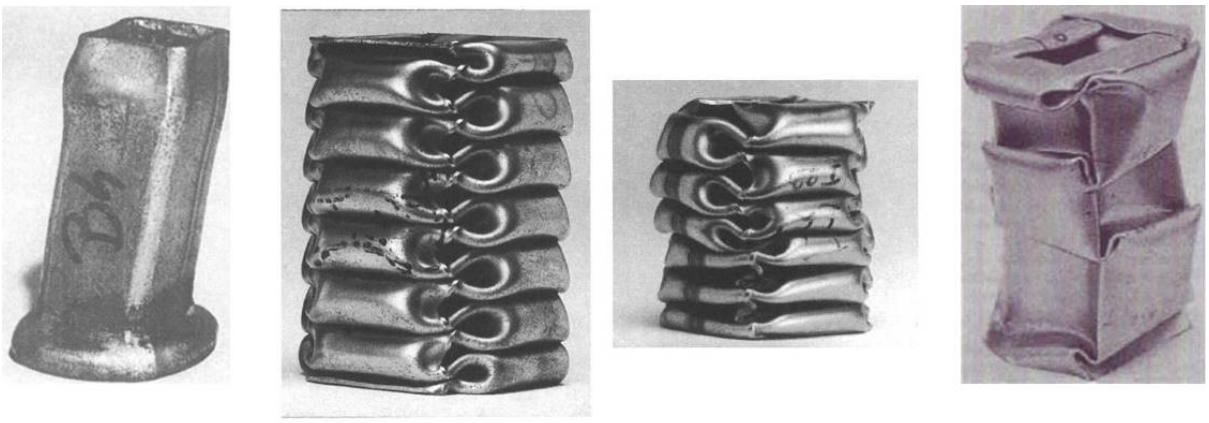

Figure 5: Global Bending deformation mode in (a) square tubes [19]- (b) circular tubes [21]- (c) Typical force–displacement responses for progressive folding and global bending of HTWEA [114].

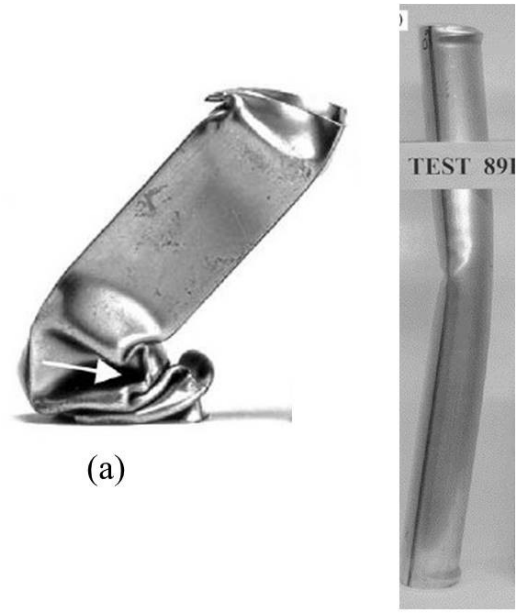

(a)

(b)

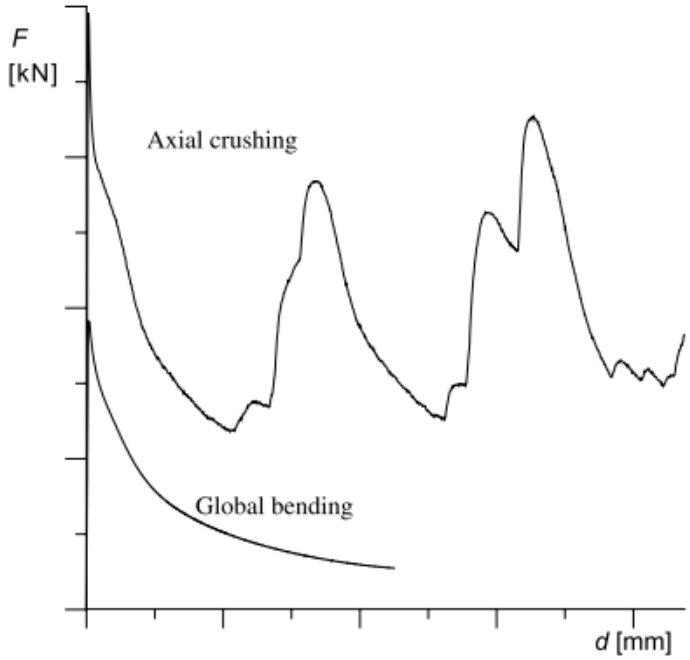

(c)

Figure 6: Illustration of multi-cell square tube with all corner and angle element [89]

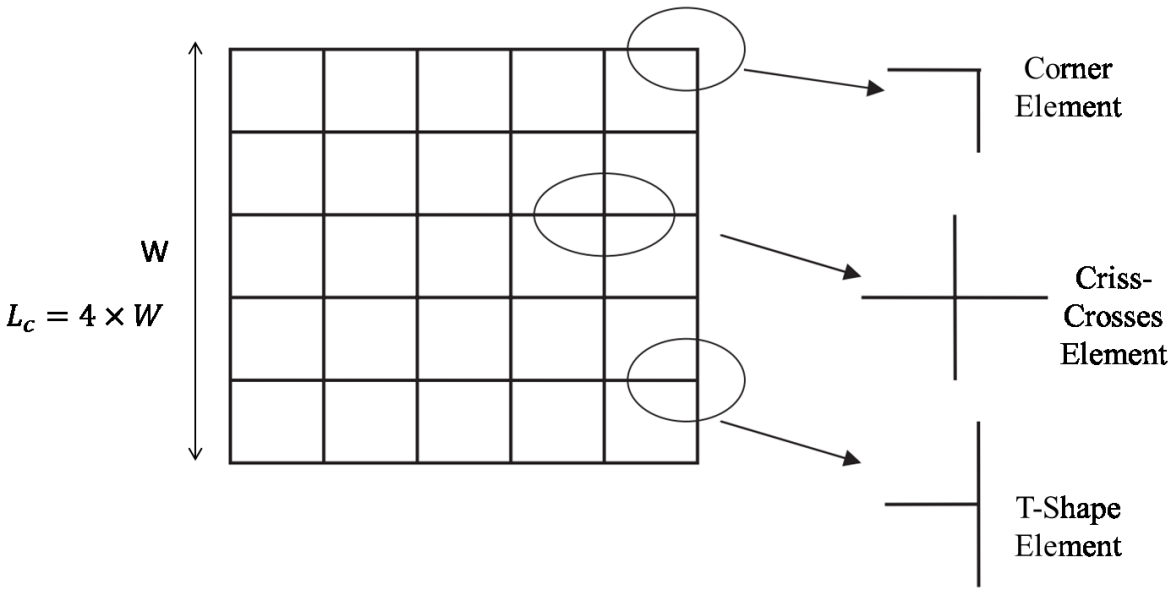

Figure 7: Various configurations of multi-cell columns studied by [91].

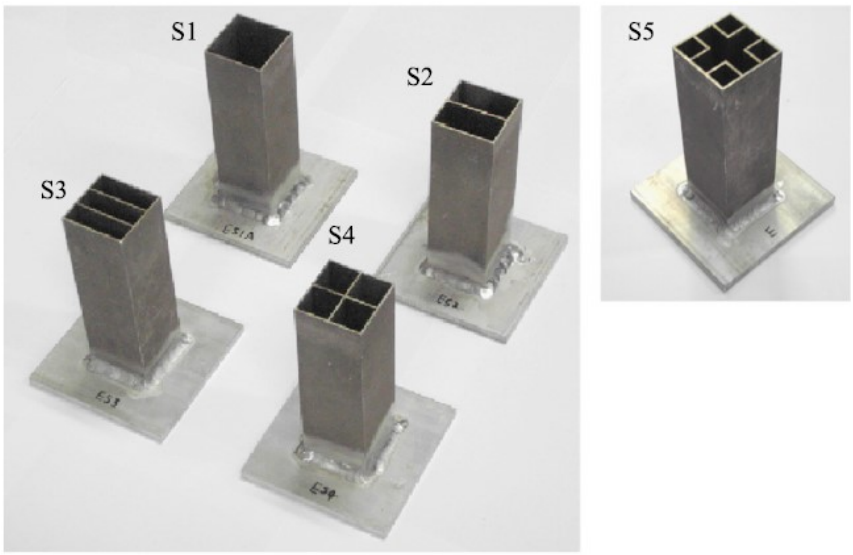

Figure 8: Schematic showing thickness gradient patterns in (a) Circular tubes (B) Square tubes

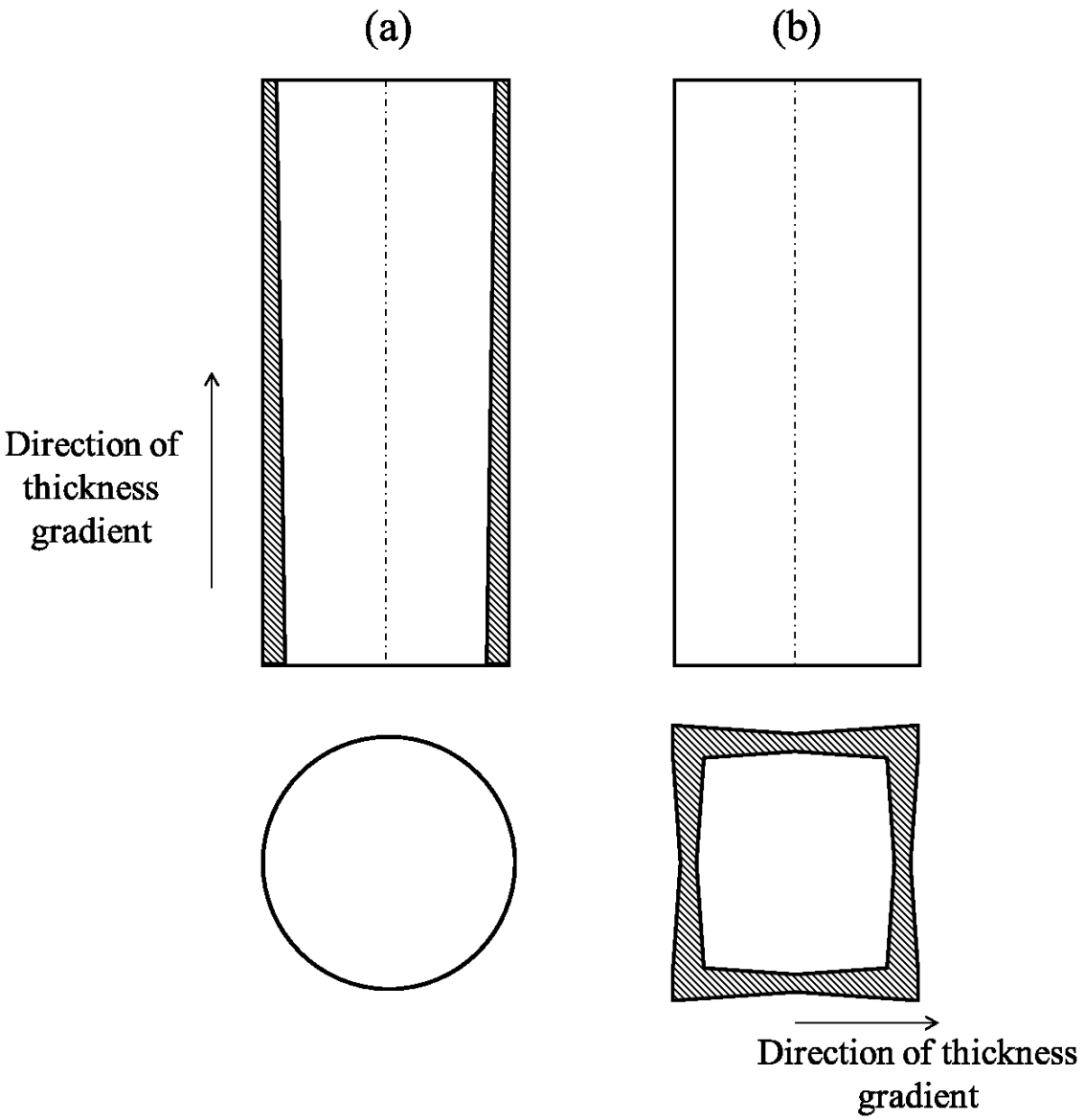

Figure 9: Bi-axially deformed (a) Square, (b) Circular tubes

Figure 10: (a) Externally stiffened tube [106], (b) laterally corrugated tube [108], (c) corrugated tube [108]

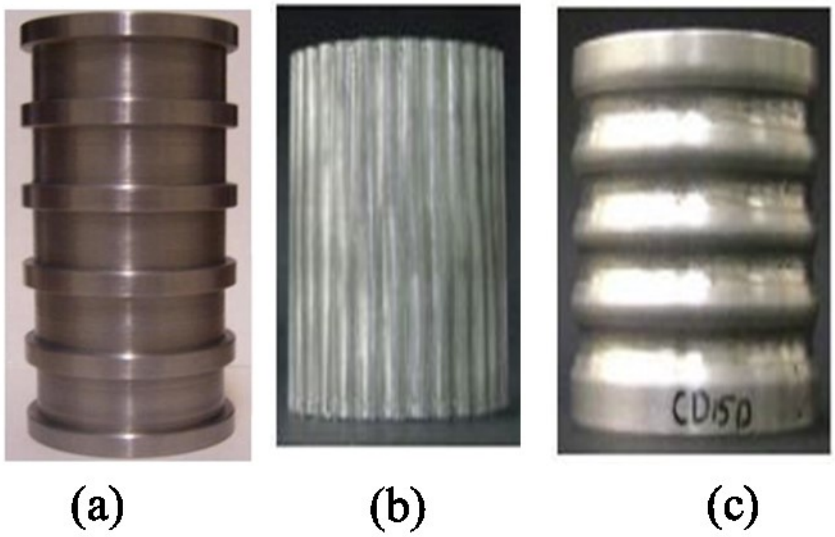

Figure 11: Deformation mode of square aluminium tube subjected to oblique loading with an angle of 5°

Figure 12: (a) Possible collapse mechanism of the circular tube under lateral loading [1] - (b) Deformed profiles of aluminium tubes at different stages of lateral compression [262].

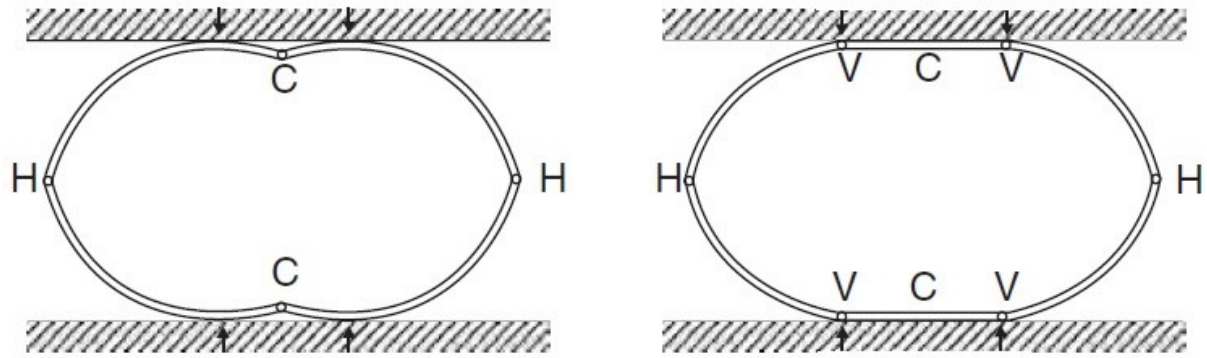

(a)

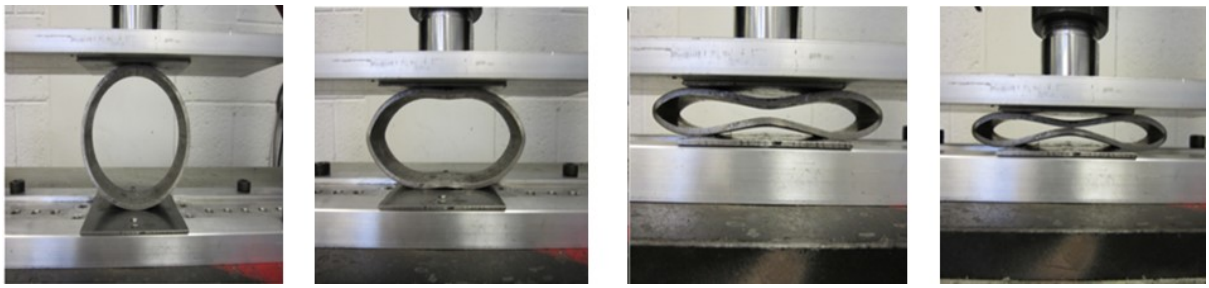

(b)

Figure 13: (a) Theoretical model of plastic deformation of rectangular under lateral loading [139] (b) Deformation history of aluminium tubes with rectangle cross section under quasi-static lateral loading [140].

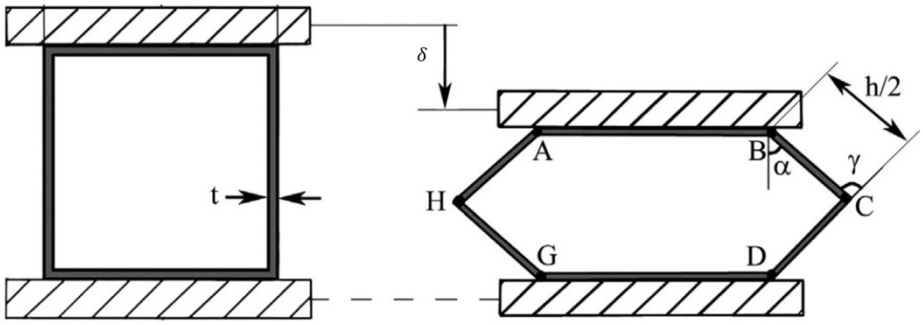

(a)

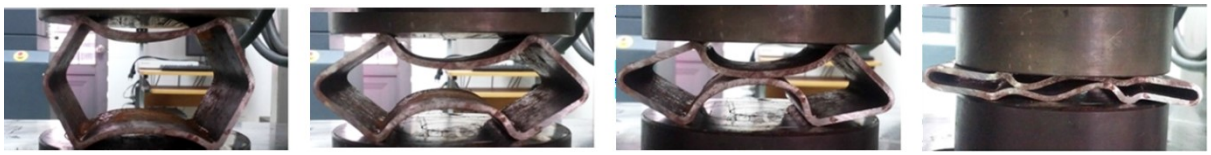

(b)

Figure 14: Preparation procedure of an oblong tube (a) initial circular tube- (b) final oblong tube [142]

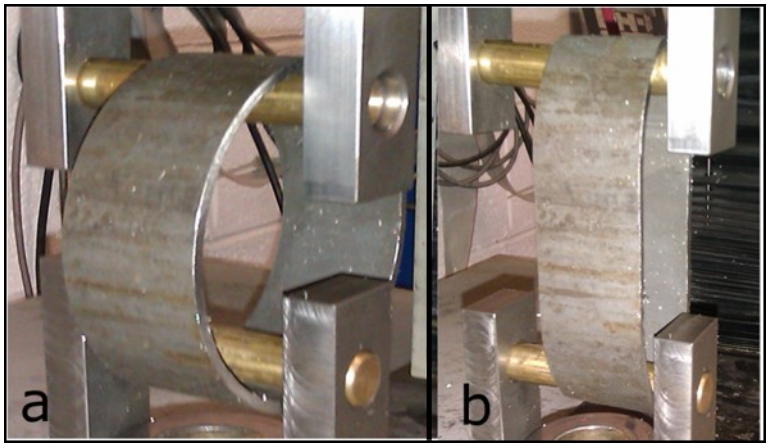

Figure 15: Collapse patterns and plastic hinges model for triangular tube under lateral loading [143]

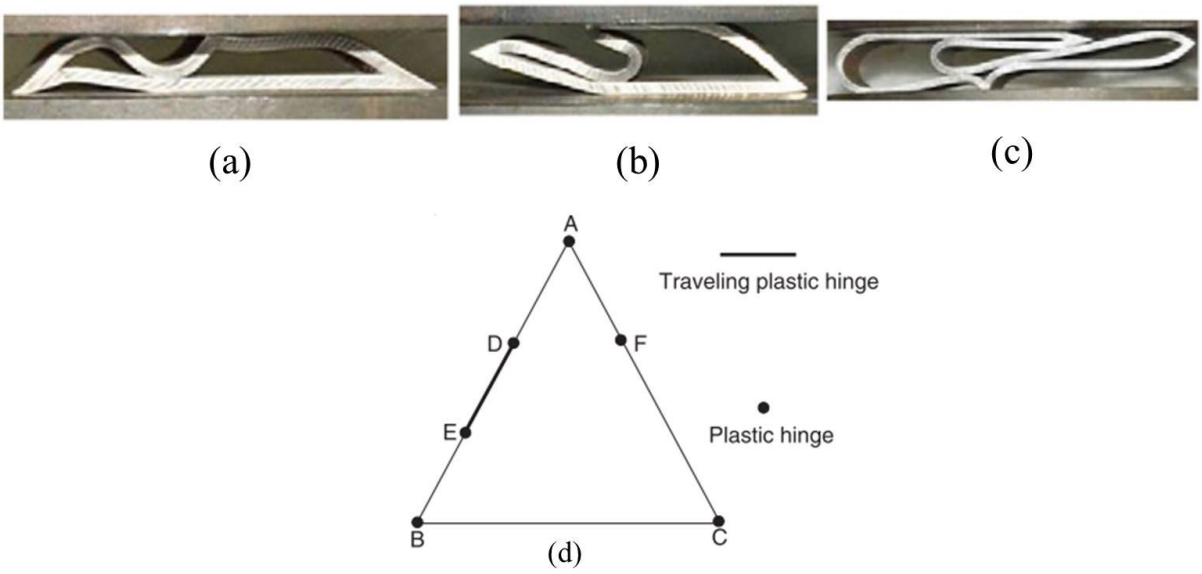

Figure 16: Various nested tubes systems under lateral loading (a) Standard nested tubes [149] (b) Optimised nested tubes [148], [151] (c) nested tubes investigated by [147] (d) Nested systems with external constraints [150]

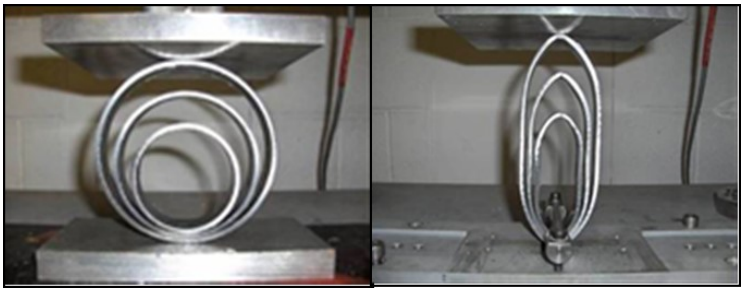

(a)

(b)

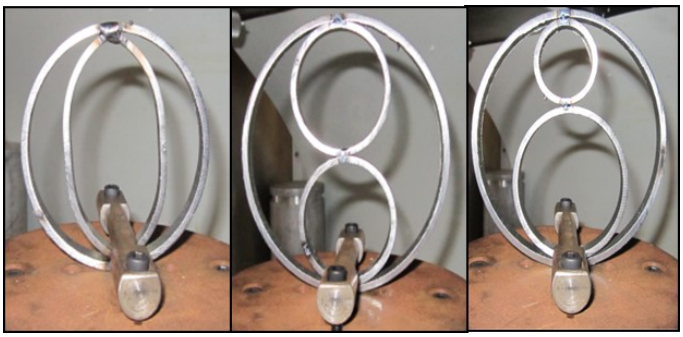

(c)

(d)

Figure 17: Deformation pattern of TW tubes under lateral bending (a) square tube [155]- (b) circular tube [212]

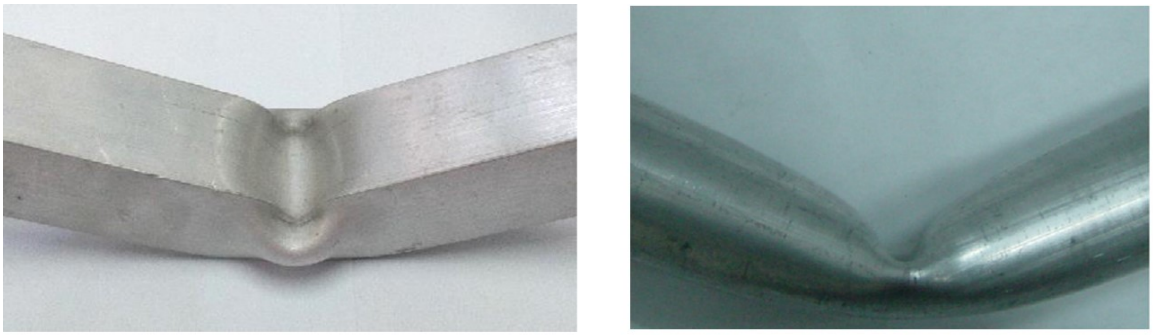

(a) (b)

Figure 18: Modelling techniques of cellular foam material

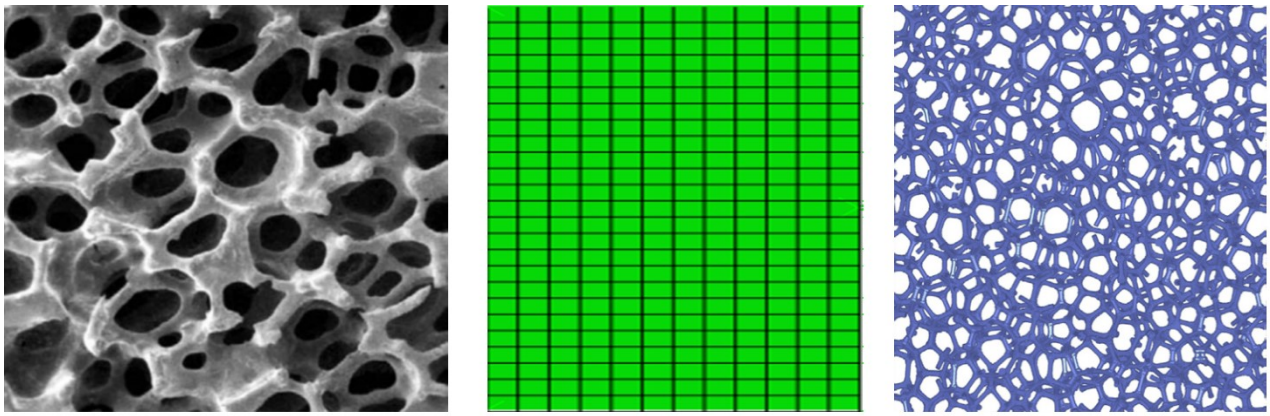

Real microstructure of foam material

Macro-mechanical model of foam material

Micro-mechanical model of foam material

Figure 19: Typical foam-filled tubes a) Foam-filled circular tubes (Al/polystyrene) [186]; -b) Foam-filled frusta [119]; -c) Foam-filled rectangle tube [182].

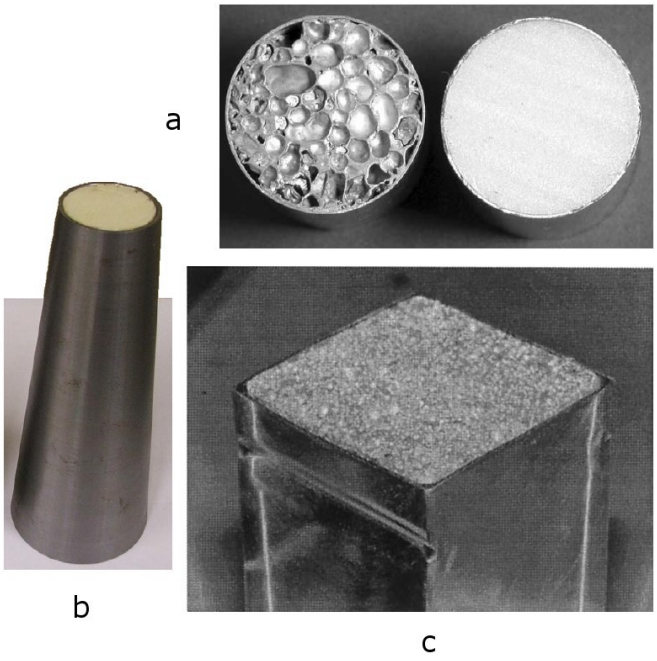

Figure 20: Deformation modes of foam-filled circular tubes [182].

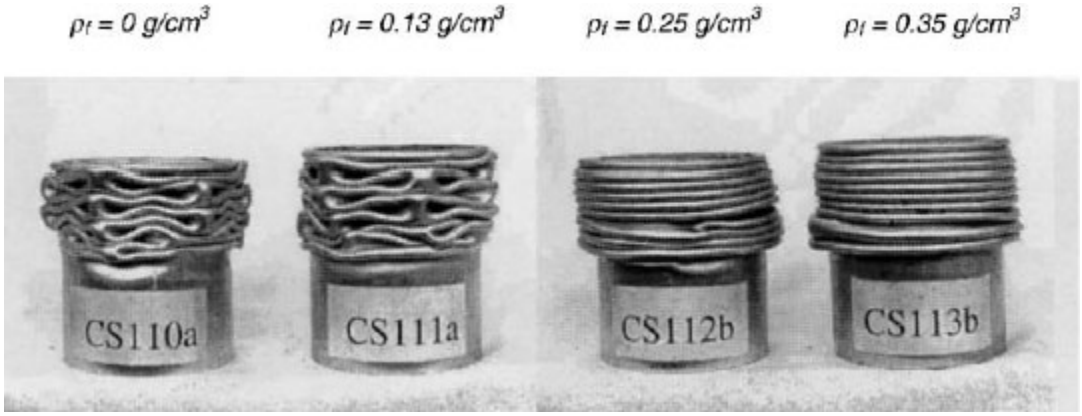

Figure 21: Concertina and diamond deformation modes foam-filled tubes and empty tubes, of three different lengths[163]

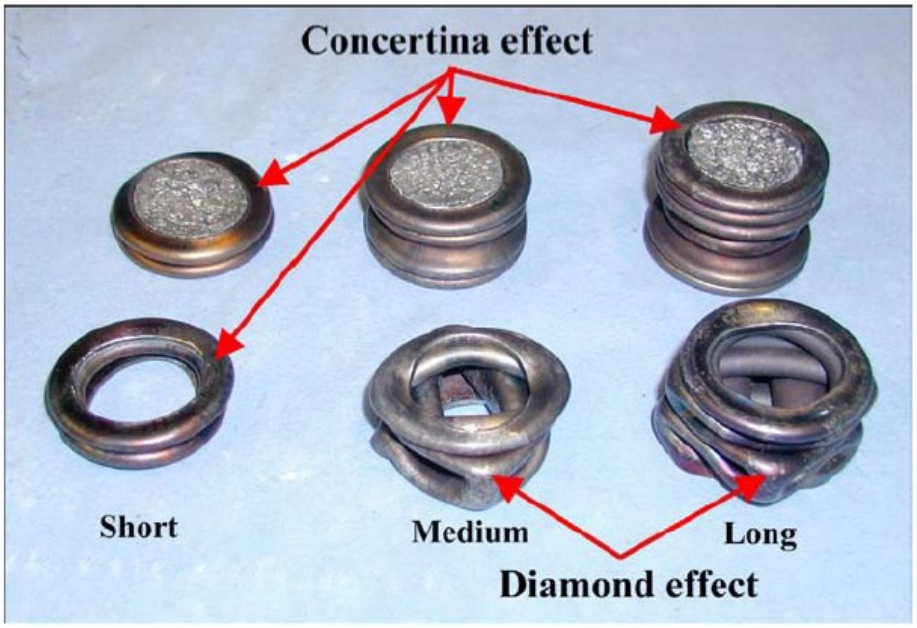

Figure 22: Interaction effect in foam-filled square tubes [185]

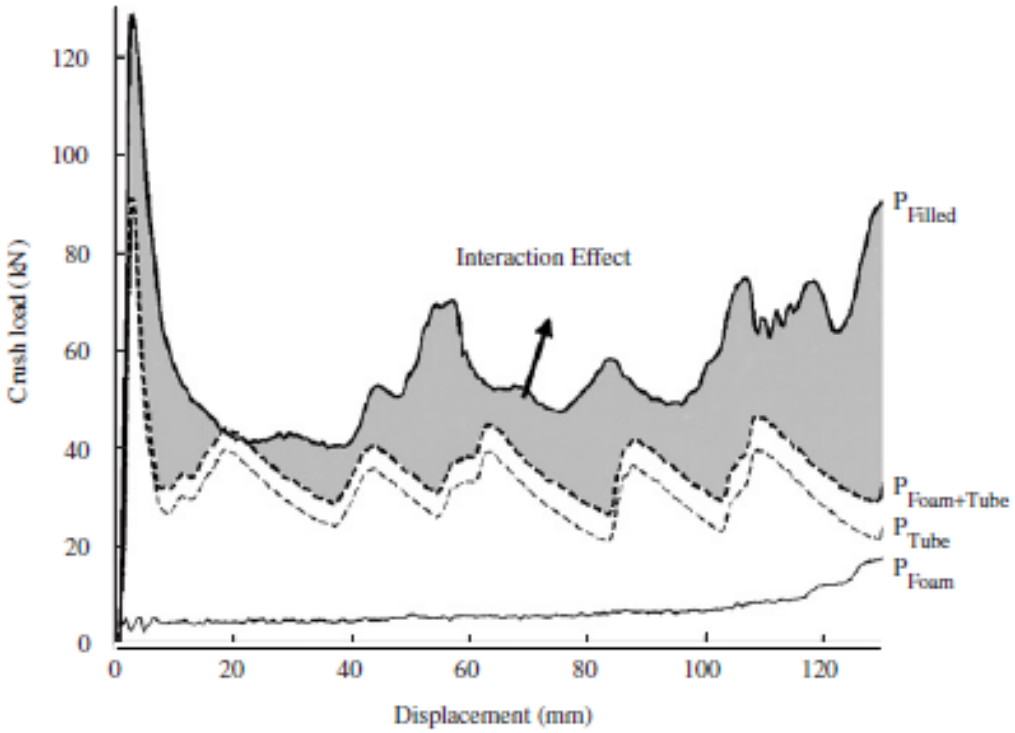

Figure 23: Global bending in axially crushed foam filled circular tubes [198].

Figure 24: Laterally crushed foam filled tubes; (a) polyurethane foam-filled Circular tube [207] - (b) polyurethane Foam-filled hexagonal tube [141]- (c) Sandwich tube with ALPORAS [205]- (d) nested foam-filled tube [209]

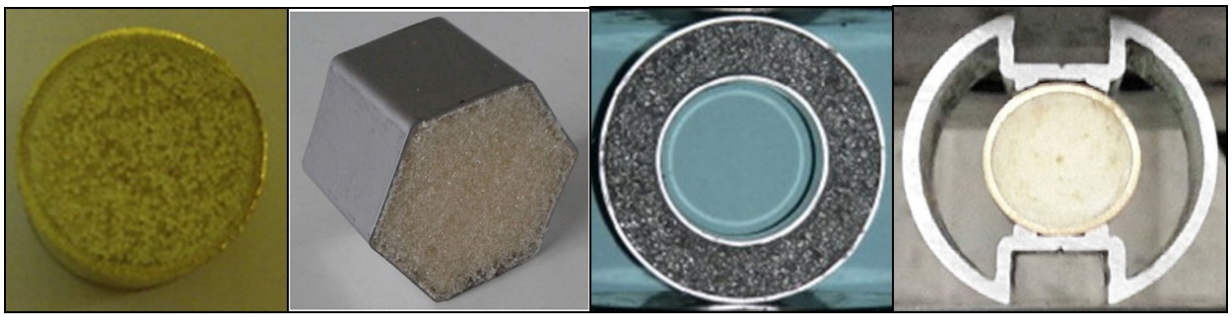

(a) (b) (c) (d)

Figure 25: Tensile failure in FFTWEA under bending loading [213]

Figure 26: Design cycle of a crashworthy structure [263]

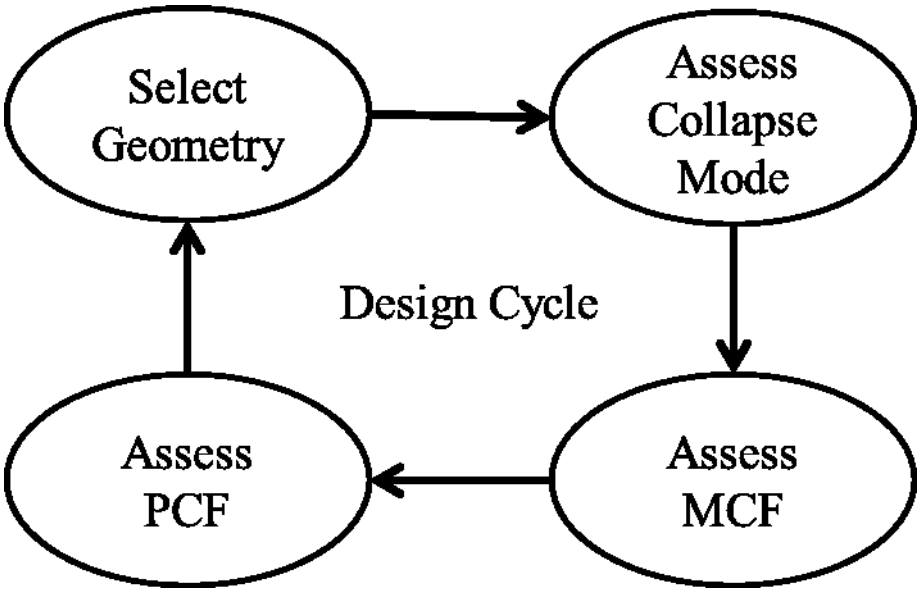

Table 1: Summary of most relevance literature on the dynamic behaviour of metals

Material	Strain rate	Summary of findings	Ref
Aluminium alloys including AA6060-T6 ,AA6082-T6, AA7003-T6 and AA7108-T6	10^{-3}-10^{3} s^{-1}	• AA6060-T6 and AA6082-T6 showed only light sensitivity to the strain rate, and can be modelled as rate-insensitive with good accuracy • AA7003-T6 and AA7108-T6 exhibited a marked sensitivity to strain rate	[264]
AA6082 and AA7108 in tempers T6 and T79	0.1-3x10^{3} s^{-1}	• Tests showed a slight increase in flow stress of the investigated alloys in the range of up to 2000 [S^{-1}]	[265]
AA7108, AA7003 and AA6060	1.5x10^{2}-1.3x10^{3} s^{-1}	• A significant influence of the strain rate on strength and strain hardening was reported	[266]
AA6005-T6	10^{-3} to 10^{3} s^{-1}	• The flow stress and ductility were found to have rather strong positive strain-rate sensitivity	[267]
AA5754 and AA5182	600,1100,1500 s^{-1}	• Both alloys exhibited significant increases in ductility with increasing the strain rate	[268]
AISI304 stainless	10^{-3} to 10^{3} s^{-1}	• AISI304 stainless was found to be strain-rate sensitive in terms of ultimate tensile strength, yielding stress, and uniform strain	[269]
Carbon steels	10^{-3} to 10^{3} s^{-1}	• Carbon steel with various percentage of C content showed positive strain-rate sensitivity	[270]
Aluminium alloy AA7075, magnesium alloy AZ80, and titanium alloy Ti–6Al–4V	0.001-5000 s^{-1}	• AA7075 and AZ80 offered high positive strain rate sensitivity in terms of ductility • Ti–6Al–4V exhibited negative strain-rate sensitivity	[271]

Table 2: Summary of crashworthiness comparative papers

Ref	Material and loading	The order of cross section from best to worst in respect to SEA capacity
[272]	• Aluminium alloy • Quasi-static loading	
[273]	• A36 steel (mild steel) • Dynamic loading	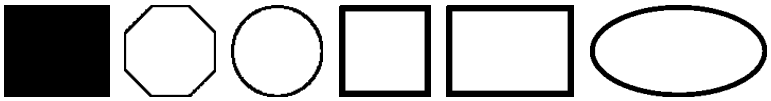
[85]	• Aluminium • Quasi-static loading	
[274]	• Aluminum • Quasi-static loading	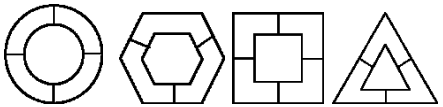

Table 3: Mean crush force of a circular tube

Ref	Deformation mechanism	Equation of Mean crush force
[51]	• Axisymmetric mode	$MCF = 6\sigma_o t^2 \sqrt{\frac{D}{t}}$
[275]	• Axisymmetric mode	$MCF = \sigma_o t \frac{6\sqrt{Dt}+3.44t}{0.86-0.57\sqrt{t/D}}$
[276]	• Asymmetric mode	$MCF = \frac{1}{4}\sigma_o t^2(-\frac{\pi}{3}N + \frac{2\pi^2}{N} tan(\frac{\pi}{2N})\frac{D}{t})$
[182]	• Asymmetric mode	$MCF = 17\sigma_o D^{1/3} t^{5/3}$

D: mean diameter of a circular tube, t: thickness

σ_o: $flow\ stress\ and\ is\ given\ by\ \sigma_o = \sqrt{\frac{\sigma_y \times \sigma_u}{1+n}}$

where σ_y: yield stress σ_u: ultimate stress, n: strain hardening exponent n from the power law stress strain curve

N: number of lobs

Table 4: Mean crush force of multi-cell tubes

Ref	Shape	Equation of Mean crush force	Gain in SEA
[99]		$MCF = 6.68\sigma_o b^{1/2} t^{3/2}$	-
		$MCF = 9.89\sigma_o b^{1/2} t^{3/2}$	18.4%
		$MCF = 12.94\ \sigma_o b^{1/2} t^{3/2}$	29.1%
		$MCF = 14.18\sigma_o b^{1/2} t^{3/2}$	41.5%
	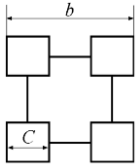	$MCF = 17.69\sigma_o (b + 2C)^{1/2} t^{3/2}$	105.1%

Table 5: Summary of most relevance literature on the dynamic behaviour of polymeric and metal foams

Material	Strain rate/Velocity	Summary of findings	Ref
Expanded polystyrene (EPS), high-density polyethene (HDPE) and rigid polyurethane (PU)	0.0087 to 2500 s^{-1}	• The EPS and HDPE materials exhibited increasing crush stress plateaus, and decreasing strain to densification, with increasing strain rate. • These effects were enhanced with increasing material density	[277]
Polyurethane foam	10^3 to $5x10^3$ s^{-1}	• The peak stress was found to be sensitive to strain-rate and depends on the square of the foam density	[278]
Aluminium alloy foams (Closed Cell Al-Mg0.6-Si0.3 and open-cell Al6101-T6)	10^{-3} -$5x10^3$ s^{-1}	• The plateau stress was reported to be strain rate insensitive	[279]
Closed-cell Hydro/Cymat aluminium foam (closed-cell: Al–Si(7–9%)–Mg(0.5–1%) alloy)	10 to 210 ms^{-1}	• For moderate strain rate, the plateau strength was found to be insensitive to the impact velocity. • For high strain rate, significant enhancement of the plateau stress was reported due to shockwave effects.	[172]
Alporas, a closed-cell aluminium foam	400 to 2500 s^{-1}	• Strain rate sensitivity was reported • The strain rate sensitivity increased with increasing the foam density	[280]
ALPORAS functionally graded aluminium foam	1000-2000 s^{-1}	• ALPORAS foam exhibited strain rate sensitivity in the range up to 1000 [S^{-1}] • For higher strain rate rates (≈ 2000 s^{-1}), the foam showed insensitive behaviour to strain rate	[281]

Table 6: Mean crush force of foam-filled tubes

Ref	Cross section	Equation of Mean crush force
[182]		$MCF = 17\sigma_o D^{1/3} t^{5/3} + \frac{\pi}{4}\sigma_f D^2 + 2.74\sqrt{\sigma_o \sigma_f} Dt$
[282]		$MCF = 13.06\sigma_o b^{1/3} t^{5/3} + \sigma_f b^2 + 5.5\sqrt{\sigma_o \sigma_f} bt$
[199]		$MCF = 14\sigma_o b^{1/3} t^{5/3} + 2\sigma_f b^2$

D mean diameter of a circular tube, *b* width of a square tube, *t* thickness

σ_o Flow stress of TW tube

σ_f Plateau stress of a foam material

Table 7: Crashworthiness metrics

Metric	Equation
Energy Absorption	$EA = \int_0^{\delta} F(x)dx$
Specific Energy Absorption	$SEA = \frac{EA}{m}$
Mean Crush Force	$MCF = \frac{EA}{\delta}$
Crush Force Efficiency	$CFE = \frac{MCF}{PCF}$
Crush Efficiency	$S_E = \frac{\delta}{l_o}$
Energy Efficiency	$E_E = \frac{MCF \times \delta}{PCF \times l_o} = CFE \times S_E$

Table 8: Summary of optimisation studies

Table legend

Hollow tube

Foam-filled tube

Multi-cell tube

Tapered tube

Tube section	Geometrical modifications				Loading				Filling Conditions					Ref
	Standard	Longitudinally Graded Thickness	Transversely Graded Thickness	Other	Axial	Oblique	Bending	Lateral	Hollow	Uniform Density Foam	Longitudinally Graded Foam	Transversely Graded Foam	Other	
	✓				✓				✓					[283], [185], [120], [246]
			✓		✓				✓					[100]
		✓			✓				✓					[243]
	✓				✓				✓					[245]
	✓				✓				✓					[246]
	✓				✓				✓					[246]
	✓				✓				✓					[246], [284]
	✓				✓				✓					[284]

	✓				✓				✓					[284]
	✓				✓				✓					[285]
			✓		✓				✓					[286]
	✓				✓				✓					[287]
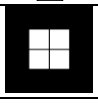	✓				✓				✓					[121]
				Indentations	✓				✓					[288]
	✓				✓				✓					[47]
	✓				✓				✓					[289]
	✓				✓				✓					[46]
	✓				✓				✓					[290], [230]
		✓			✓				✓					[242]
				Stiffeners		✓			✓					[238]
				Corrugations		✓			✓					[291]
		✓			✓				✓					[292]
				Indentations	✓				✓					[293]
				Cut-outs	✓				✓					[113]
	✓				✓					✓				[294], [185], [245], [120], [221], [295], [104]
	✓				✓						✓			[220], [221]

	✓				✓							✓		[295]
			✓		✓					✓				[104]
			✓		✓							✓		[225]
	✓				✓					✓				[245]
	✓				✓						✓			[220]
	✓				✓						✓			[220]
	✓				✓						✓			[220]
	✓				✓						✓			[220]
	✓				✓					✓				[296]
	✓				✓						✓			[220]
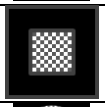	✓				✓					✓				[297]
		✓			✓					✓				[101]
	✓				✓					✓				[249], [298]
	✓				✓								Honeycomb	[227]
	✓				✓					✓	✓			[222]
	✓					✓			✓					[120]
	✓					✓			✓					[121]
	✓					✓			✓					[46]
	✓	✓				✓			✓					[299]
	✓					✓			✓	✓				[118]
	✓					✓				✓				[120]

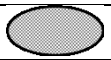	✓					✓			✓	✓				[202]
		✓				✓				✓				[101]
	✓					✓			✓	✓				[118]
			✓				✓		✓					[155]
				Ribs			✓		✓	✓				[157]
		✓					✓		✓					[156]
	✓						✓			✓				[210], [104]
			✓				✓			✓				[104]
	✓						✓					✓		[300]
	✓						✓			✓				[301]
	✓						✓		✓					[302]
	✓							✓	✓					[129]
	✓							✓	✓					[142]
	✓							✓		✓				[45]